Palacio, Carlos; Mayerle, Roberto; Toro, Mauricio; Jimenez, Nestor

Modelling of Flow in a Tidal Flat Area in the South-Eastern German Bight

Die Küste

Die Küste, 69 PROMORPH (2005), 141-174

Modelling of Flow in a Tidal Flat Area in the South-Eastern German Bight

By CARLOS PALACIO, ROBERTO MAYERLE, MAURICIO TORO and NESTOR JIMÉNEZ

Summary

This paper sums up the development phases of a flow model for a tidally-dominated area of the German North Sea. The study area is the Dithmarschen Bight located between the Elbe and Eider estuaries. The model presented is a two-dimensional depth-integrated flow model based on the DELFT3D Modelling System developed by Delft Hydraulics in the Netherlands. A description of model set-up as well as the results of sensitivity studies and model calibration and validation procedures are outlined in this contribution. Measurements of water levels and current velocities with a dense spatial and temporal coverage were used for this purpose. It was found that hydrodynamic forcing along the open sea boundaries is by far the most important factor governing the predictive capability of the model. Sensitivity studies indicated that the effect of seasonal bathymetric changes on current velocities may be quite significant. The effect of spatially variable bed roughness on the flow field was found to be less significant. The validation results showed that the model is capable of reproducing water levels and current velocities in the study area in fair agreement with observations. The mean absolute errors between computed and observed water levels at a number of locations covering periods of several months were found to be less than 10 cm (3 % of the mean tidal range) and 20 cm (6 % of the mean tidal range) at high and low water levels, respectively. The mean absolute errors between computed and observed depth-averaged velocities at various cross-sections in the tidal channels were generally found to be less than 0.2 m/s, which represents less than 20 % of the tidally-averaged value. The model simulation results indicated a certain tendency towards underestimation of current velocities in the tidal channels. On the basis of the quality standards usually adopted (WALSTRA et al., 2001 and VAN RIJN et al., 2002), the performance of the model with regard to current velocity predictions was found to range between good and excellent.

Zusammenfassung

Dieser Beitrag fasst die Entwicklungsphasen eines Strömungsmodells für ein tidedominiertes Gebiet, Deutsche Nordsee, zusammen. Untersuchungsgebiet ist die Dithmarscher Bucht zwischen Elbe- und Eiderästuar. Auf Grundlage des DELFT3D Modellsystems von Delft Hydraulics (Niederlande) wurde ein 2-dimensionales tiefenintegriertes Strömungsmodell entwickelt. Beschrieben werden Modellaufbau, Ergebnisse der Sensitivitätsstudien sowie Modellkalibrierung und Validierung. Hierzu wurden Messungen von Wasserständen und Strömungsgeschwindigkeiten mit dichter zeitlicher und räumlicher Deckung verwendet. Es stellte sich heraus, dass der hydrodynamische Antrieb auf Grundlage der Wasserstände entlang der Offene-See-Grenzen den bei weitem signifikantesten Faktor für die Vorhersagefähigkeit des Modells darstellte. Signifikanztests ergaben, dass Effekte saisonaler bathymetrischer Veränderungen für die Strömungsgeschwindigkeit durchaus signifikant sein können. Es zeigte sich, dass räumlich variable Bodenrauheiten für die Ausprägung des Strömungsfelds weniger signifikant waren. Die Ergebnisse der Validierung zeigten, dass das Modell in der Lage ist, Wasserstände und Strömungsgeschwindigkeiten im Untersuchungsgebiet in recht guter Übereinstimmung mit den Beobachtungen zu reproduzieren. Die mittleren absoluten Fehler zwischen den simulierten und den an mehreren Orten über mehrere Monate gemessenen Wasserständen lagen bei Hochwasser unter 10 cm (entsprechend 3 % des mittleren Tidehubs) und bei Niedrigwasser unter 20 cm (entsprechend 6 % des mittleren Tidehubs). Die mittleren absoluten Fehler zwischen simulierten und den in verschiedenen Querschnitten der Gezeitenrinnen gemessenen tiefenintegrierten Geschwindigkeiten lagen unter 0,2 m/s, entsprechend weniger als 20 % des tidegemittelten Wertes. Die Simulationsergebnisse zeigen eine *gewisse Tendenz, die Strömungsgeschwindigkeiten in den Gezeitenrinnen zu unterschätzen. Legt man den Ergebnissen die normalerweise angewandten Qualitätsstandards (*WALSTRA *et al., 2001;* VAN RIJN *et al., 2002) zugrunde, so lag die Leistung des Modells für Vorhersagen der Strömungsgeschwindigkeit zwischen gut und sehr gut.*

Keywords

Coastal Flow Models, Sensitivity Analysis, Model Calibration, Model Validation, Open Sea Boundaries, Field Measurements, PROMORPH, North Sea, Dithmarschen Bight.

Contents

1. Introduction

Process-based models for simulating flow, waves, sediment transport and morphological evolution have been developed within the framework of the research project "Predictions of Medium-Scale Morphodynamics – PROMORPH" funded by the German Ministry of Education and Research (BMBF) over the period 2000 to 2002. The research project was motivated by the need to predict morphological changes in a tidally-dominated area on the German North Sea coast over periods of several years.

This paper sums up the development phases of a flow model for the central Dithmarschen Bight (see Fig. 1). The model implements a two-dimensional depth-integrated (2DH) flow model solver developed by Delft Hydraulics in the Netherlands. The results of model set-up, sensitivity studies, calibration and validation are presented. The variability of the computed water levels and current velocities relative to the main physical and numerical parameters was investigated at several monitoring stations. The model was calibrated and validated using water level recordings at a number of gauge stations over a period of several months and current velocities measured over several cross-sections in the main tidal channels in order to cover the full range of tidal and meteorological conditions typical of the study area. The performance of the model was determined quantitatively on the basis of a set of statistical parameters. The results of an evaluation of the predictive capability of the model with regard to water levels and current velocities are also presented.

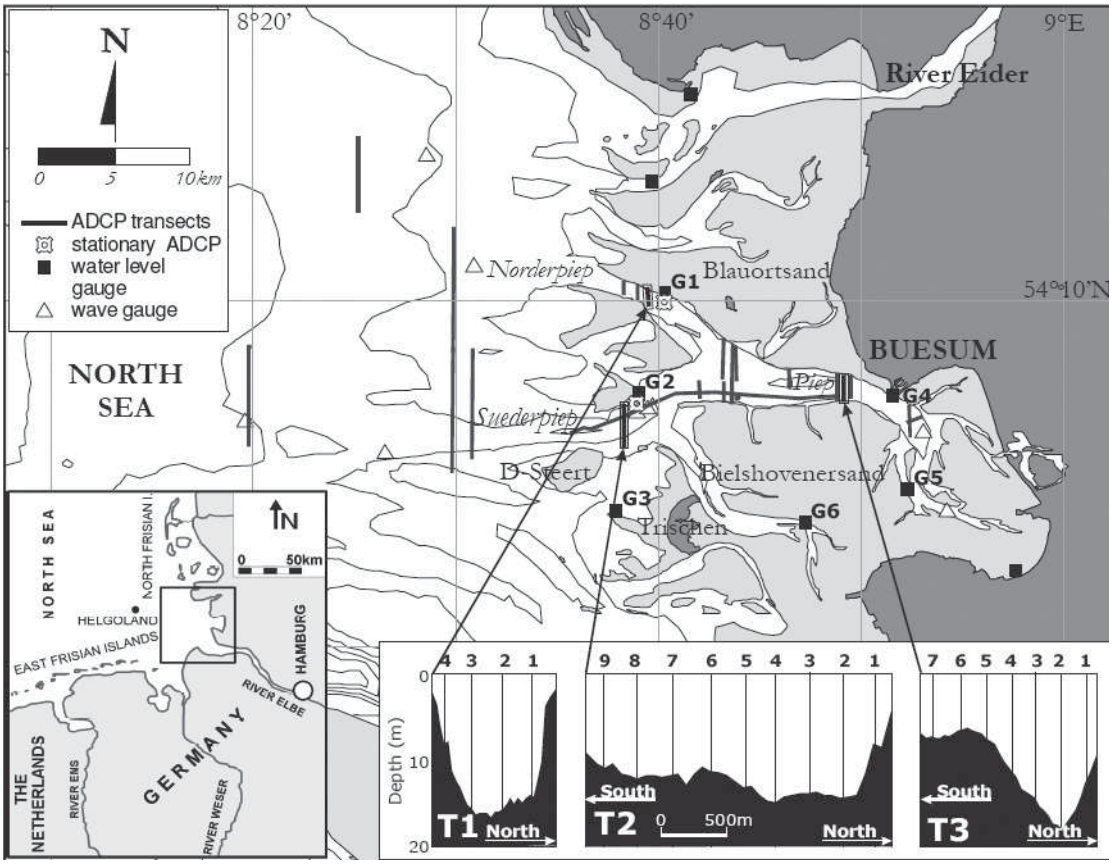

Fig. 1: Investigation area showing surveyed cross-sections and gauge stations

2. Description of the Study Area

The study area is located about 100 km north of Hamburg between the Eider and Elbe estuaries. The morphodynamics of the study area are dominated by tidal flats and a tidal channel system comprised of three channels: the Norderpiep in the northwest, the Suederpiep in the southwest, and the Piep tidal channel, which is formed at the confluence of the Norderpiep and Suederpiep. Under normal conditions the maximum mean water depth in the tidal channels is about 18 m. The tidal flats and sandbanks are exposed at low water. The area is characterized by a meso-tidal regime with a mean tidal range of 3.2 m and neap and spring tidal ranges of about 2.8 m and 3.5 m, respectively. The current velocities in the tidal channels attain maximum values of about 2.8 m/s (TORO et al., in this volume). The small bed forms and correspondingly low bed roughness coefficients are responsible for the generally fairly uniform distribution of velocities over the vertical (MAYERLE et al., in this volume(a)).

With regard to the wave and wind climate, the study area is classified as a storm wave environment with prevailing westerly winds (SW-W). Although wave heights in the outer region may attain 3 to 4 m, these break along the edge of the tidal flats (margins) of the investigation area. Despite the absence of barrier islands, intertidal and supratidal sandbanks in the outer regions prevent the penetration of waves into the tidal flat area. Small wind-generated waves of up to about 0.5 m in height are observed in the study area (TORO et al., in this volume). The influence of local waves on currents is moderate over the tidal flats and negligible in the tidal channels. Storm surges may produce water level set-ups of up to 5 m, favouring the propagation of waves into shallow regions. Even under such conditions, however, wave effects are mostly confined to the outer sandbanks. The seabed sediment in the tidal channels and on the tidal flats consists mainly of sands with varying proportions of silt and clay (RICKLEFS and ASP, in this volume). The grain sizes of sediment transported in suspension are much finer than those of seabed sediment (POERBANDONO and MAYERLE, in this volume).

3. Flow Model

Several models for simulating flow, sediment transport and morphological evolution have been developed in the past for the Dithmarschen Bight (HARTSUIKER, 1997; HIRSCHHÄUSER and ZANKE, 2001). Due to a lack of field data, however, very little is known about the performance of the models, particularly regarding the quality of simulated current velocities.

The simulations carried out in the present study were performed using the two-dimensional depth-integrated (2DH) DELFT3D flow model developed by Delft Hydraulics in the Netherlands. This model solves the non-steady depth-integrated momentum and continuity equations for depth-integrated velocities and water levels. The implicit scheme adopted for the time integration enables simulations to be performed for Courant numbers as high as 10. An algebraic approach for turbulence closure using a constant value of eddy viscosity was adopted (ROELVINK and VAN BANNING, 1994).

The set-up procedure for the flow model includes in the definition of the model limits, the construction of a grid system, and preliminary runs to detect spurious oscillations was done initially. Fig. 2 shows the bathymetry and limits of the flow models implemented in the present investigation. Details of the models developed in this study are given in Table 1. Preliminary investigations to check the global behaviour of the model system as well as sensitivity studies were only carried out for the model covering the central Dithmarschen Bight (CDBM). As the sandbanks and entrances to the main tidal channels are subject to intensive morphological changes, the western open sea boundary of the CDBM was extended a further 15 km seawards to yield the Extended Central Dithmarschen Bight Model (ECDBM). Finally, a model covering the entire bight with the inclusion of the Elbe and Eider estuaries was set-up. This larger model is referred to as the Dithmarschen Bight Model (DBM). The open sea boundaries are located in deeper water at a fair distance from the region of interest (see also Fig. 3).

The bathymetry used to set up the models was based on measurements made in 1998 by the Federal Maritime and Hydrographic Agency (BSH) in Hamburg. The bathymetry of the tidal flat regions was obtained from bathymetric maps drawn up in 1990 by the Office for Rural Development in Husum. The effect of bathymetry on computed water levels and current velocities was investigated for the reference grid (as defined in Section 4) based on bathymetric measurements made in 1990, 1996 and 1998 covering the Central Dithmarschen Bight. The curvilinear grids adopted for model computations were appropriately matched to the bathymetry of the various model domains. Due to the fact that the numerical errors in the cross-advection term of the DELFT3D flow model are proportional to the orthogonality value, the orthogonality of the grids was kept as low as possible.

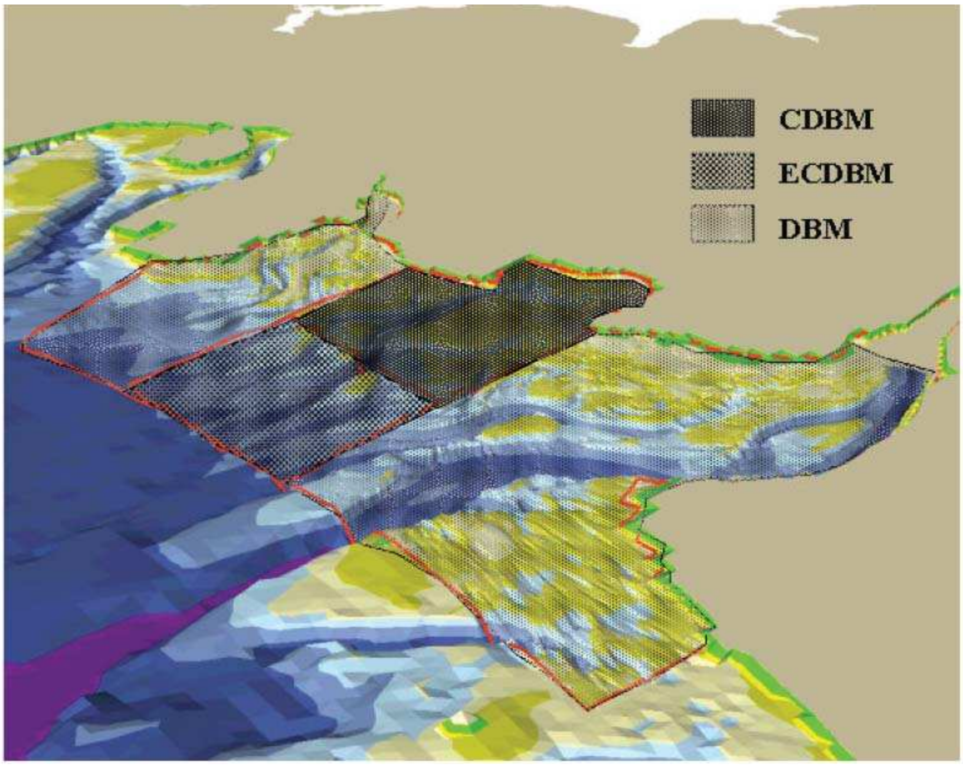

Fig. 2: Perspective view of the study area showing bathymetry and the limits of the flow models

Table 1: Details of the flow models

	Central Dithmarschen Bight Model (CDBM)	Extended Central Dithmarschen Bight Model (ECDBM)	Dithmarschen Bight Model (DBM) – Fig. 3
Dimensions (km)	20 by 17	35 by 17	37 by 54
Area (km^2)	300	520	1640
Seaward boundary	14 km west of Buesum	29 km west of Buesum	29 km west of Buesum
Grid spacing	60 × 180 m	90 × 150 m	80 × 200 m
No. of Grid Cells	30,000	36,000	43,250

The flow model is driven by the combined effects of hydrodynamic forcing along the open sea boundaries and winds. Each of the models has three open sea boundaries, i.e. a western, northern and southern boundary (see Fig. 2). The flow field in the central Dithmarschen Bight is mainly governed by the tidal wave propagating through the western seaward boundary. The northern and southern open sea boundaries of the CDBM are located on the tidal flats, which fall dry during low tide. As the latter boundaries are far removed from the region of interest, their effect on flow conditions in the central Dithmarschen Bight is negligible. For the purpose of hydrodynamic forcing in the present study, water levels were specified along the western open sea boundaries. Along the open boundaries of the Elbe and Eider estuaries, flow discharges were specified.

Wind fields were obtained with the aid of the PRISMA interpolation model developed by the Max Planck Institute of Meteorology in Hamburg (LUTHARDT, 1987). This model generates synoptic wind fields from a large set of measurements at locations along the coastline and at offshore stations covering the entire North Sea. The data is generated every three hours with a spatial resolution of 42 km. A comparison of the PRISMA model results with wind measurements made by the Research and Technology Centre Westcoast of the University of Kiel over a period of 8 years confirmed the high quality of the PRISMA model results (WILKENS, 2004). Wind data generated by the PRISMA model were interpolated in time and space to provide the required information for driving the flow model of the investigation area.

After completing the flow model set-up procedure, flow simulations were carried out using "standard" physical and numerical parameters in order to detect spurious velocity fields and anomalous water level contours due to incorrect settings. The model simulations were found to yield smooth water levels, smooth and realistic velocity fields, and no spurious circulation patterns.

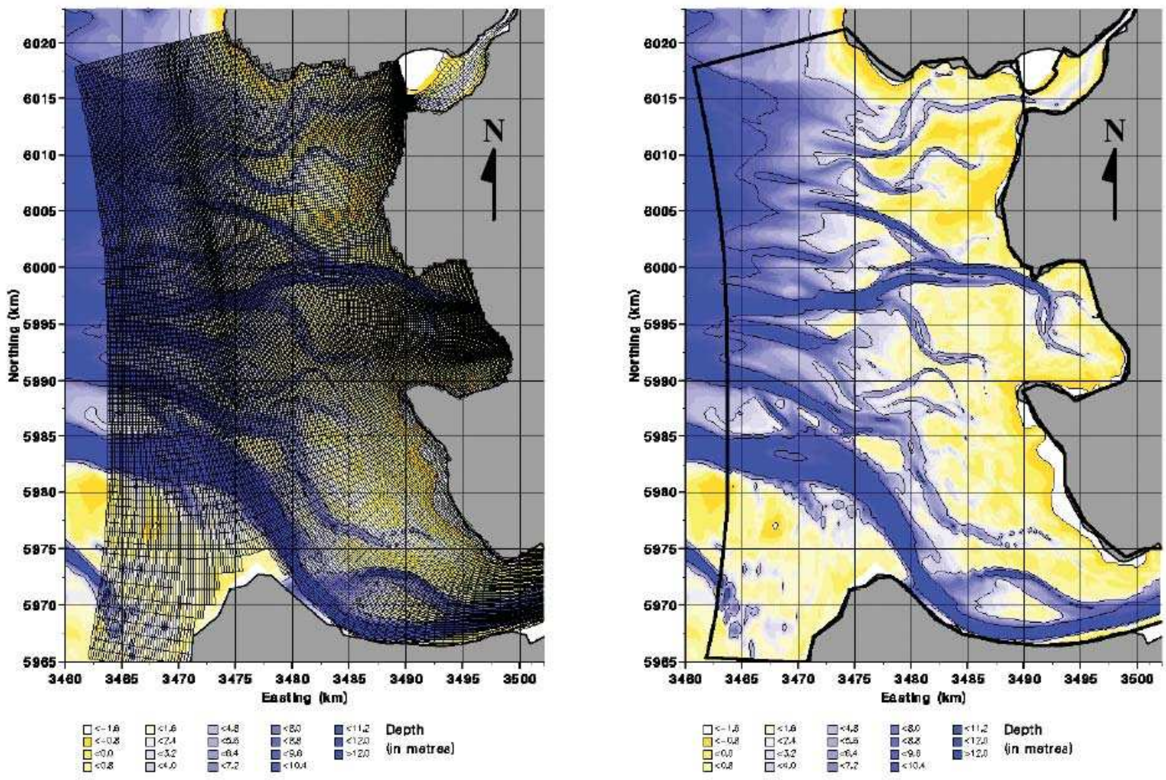

Fig. 3: Bathymetry and curvilinear grid of the DBM

4. General Model Behaviour and Sensitivity Studies

The purpose of sensitivity studies is to gain an understanding of the overall behaviour of a model and its response to changes in the physical and numerical parameters adopted. On the basis of a sensitivity analysis it is also possible to identify the particular physical parameters that have a predominant effect on computed water levels and current velocities.

The sensitivity analysis was carried out at several locations throughout the study area for a variety of situations representative of the main flow conditions, i.e. for different tidal phases and tidal periods as well as for different meteorological conditions. A plan view of

Die Küste, 69 PROMORPH (2005), 141-174

the CDBM indicating the defined cross-sections and monitoring stations selected for the sensitivity analysis is shown in Fig. 4. The variability of computed water levels and velocities at the selected monitoring stations was investigated in relation to the computational time step, grid resolution, various approaches for defining hydrodynamic forcing along the open sea boundaries, wind speed and direction, bottom roughness, eddy viscosity and bathymetry. Moreover, the influence of waves on currents and the relevance of a three-dimensional model approximation were also investigated. The analysis was carried out on the basis of comparisons of computed water levels and velocities obtained at the monitoring stations over a three-day simulation period (May 18 to May 21, 1999) for different model settings and parameters. The results of sensitivity tests for grid spacing, bed roughness, influence of waves and relevance of 3D model approximations and morphology are presented. The results of sensitivity tests with respect to the remaining parameters are summarized in PALACIO et al. (2003).

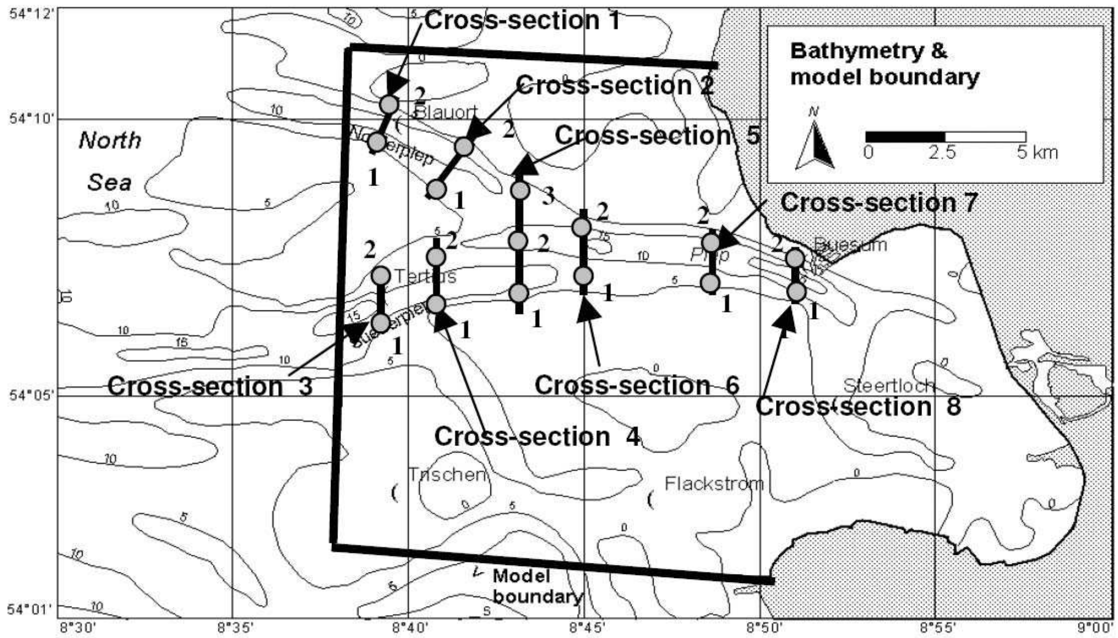

Fig. 4: Selected cross-sections and monitoring stations for the sensitivity analysis

With regard to the computational grid, the mesh size should be sufficiently small to correctly reproduce hydrodynamic conditions in the study area and at the same time permit simulations of coupled flow, wave and sediment transport processes for the purpose of modelling morphological evolution. Investigations of the effect of grid spacing on flow conditions were carried out considering three grid systems: a) a reference grid with a mesh size ranging from 60 m to 180 m; b) a fine grid with a mesh size ranging from 30 m to 90 m and c) a coarse with a mesh size ranging from 120 m to 360 m. Fig. 5 shows the grid resolution of the three grids. The reference grid with about 30,000 cells was initially generated and the fine and coarse grids were subsequently obtained by refining and coarsening the reference grid once in each case. The DBM incorporating these different grid resolutions is also shown in Fig. 5 together with a comparison between the modelled bed profile given by the three different grids and the measured bed profile over cross-section A-A at the intersection of the Norderpiep, Suederpiep and Piep tidal channels. As is evident in the figure, the coarse grid is unable to adequately describe the measured bathymetry. The volumetric consistency of the model for the different grids was checked by comparing the volumes calculated below a defined reference level for the three grid systems with the volume computed from bathymetric measurements. This check resulted in only minor volumetric differences. In the case of the coarse grid, however, discrepancies were observed between computed and measured water levels and current velocities throughout the domain. The largest velocity discrepancies given by the coarse grid were found in cross-section 7 (see Fig. 6). Based on the results of this analysis it was concluded that the reference grid is quite adequate for realistically reproducing hydrodynamic conditions in the modelled domain.

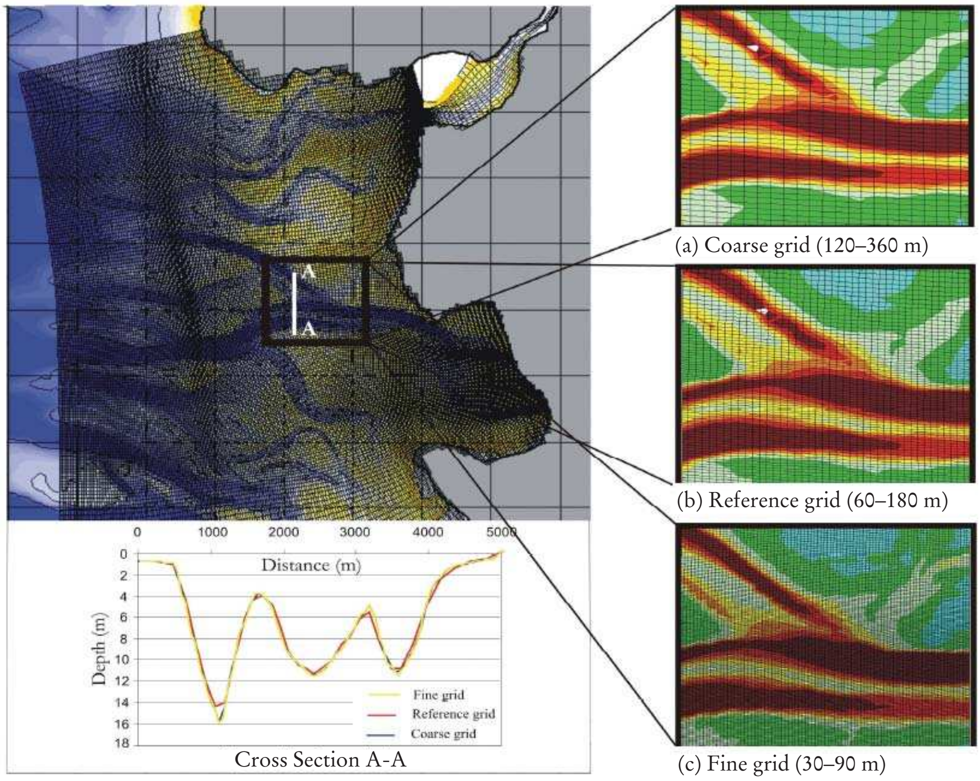

Fig. 5: Grid resolutions showing a comparison between the modelled and measured depth profile over cross-section A-A

The response of the flow model to changes in the bed roughness was investigated by varying the Chézy coefficient throughout the modelled domain. Constant temporal and spatial values of 40 $m^{1/2}/s$, 50 $m^{1/2}/s$ and 60 $m^{1/2}/s$ were considered for this purpose. As indicated in Fig. 7, the bottom roughness has a clear influence on the computed depth-averaged velocities. This effect is more pronounced in the case of the highest roughness value. Small phase shifts also resulted in the computed water levels, which were found to be most pronounced in cross-sections near the coastline. As the highest roughness value of 60 $m^{1/2}/s$ yielded the best results in overall terms, this value was adopted for model calibration. A detailed investigation of the spatial and temporal variations of the dimensions of bed-form features and associated bed roughness values based on field measurements is given in MAYERLE et al. (in this volume(a)), which also includes roughness maps accounting for the layer thickness of potentially mobile sediments, the characteristics of superficial seabed sediments and local flow conditions.

In view of the intense morphological activity observed at various locations in the study area, the influence of bathymetry on computed water levels and velocities was also investigated throughout the domain. In order to permit a better evaluation of bathymetric variations over shorter periods a monitoring programme was set up. Within the scope of this programme the bed profiles of cross-sections T1, T2 and T3 were surveyed between June 2000 and August 2003 (see ASP, 2004 and RICKLEFS and ASP, in this volume). As a result, it was found that changes in the bed profiles can be quite significant, especially in the most exposed areas such as, e.g. over cross-sections T1 and T2 in the Norderpiep and Suederpiep tidal channels, respectively (see Fig. 1). Bathymetric changes of up to 4–5 m were observed in these cross-sections during the period of measurements. Although cross-section T3 in the Piep tidal channel proved to be fairly stable, bathymetric changes of up to 2–3 m were observed in this cross-section. For the purpose of investigating the effect of bathymetry on computed flow values the reference grid was adjusted to match three different bathymetries based on measurements made in 1990, 1996 and 1998. The computed volumetric *percentage differences* between the model bathymetries of 1990 and 1996 and the model bathymetry based on 1998 measurements revealed only minor differences (0.73 % and 0.03 % respectively). Similarly, the results of model simulations using the three bathymetries mentioned above yielded only slight differences in computed water levels. With regard to depth-averaged current velocities, on the other hand, differences of up to 0.2 m/s were obtained at a number of monitoring stations (see Fig. 8). The fact that seasonal variations in the bathymetry of the tidal channels can be quite significant stresses the importance of updating the model bathymetry regularly.

Investigations of the effects of wind and waves on currents were also carried out. With regard to wind conditions it was found that wind speeds below 8 m/s have little influence on the model results. In order to assess the influence of waves on currents, simulations were carried out using a coupled flow and wave model. Details of the wave model are presented in WILKENS et al. (in this volume). Wave simulations were performed using the DBM for wave heights ranging between 1 m and 3 m along the open sea boundary. Comparisons between computed current velocities with and without wave influence were made at a position located in a shallow channel on Tertiussand and at a location near Buesum. Under these conditions, wave heights of up to 3 m were computed on the western boundary, resulting in differences of about 0.10 m/s in depth-averaged flow velocities. At the monitoring station near Buesum, on the other hand, the differences in computed flow velocities were generally found to be negligible due to large local depths and smaller wave heights at this location. A noticeable difference was observed, however, during slack water. It may be concluded from these results that the effect of waves on depth-averaged currents is negligible in the tidal channels for the wave conditions considered.

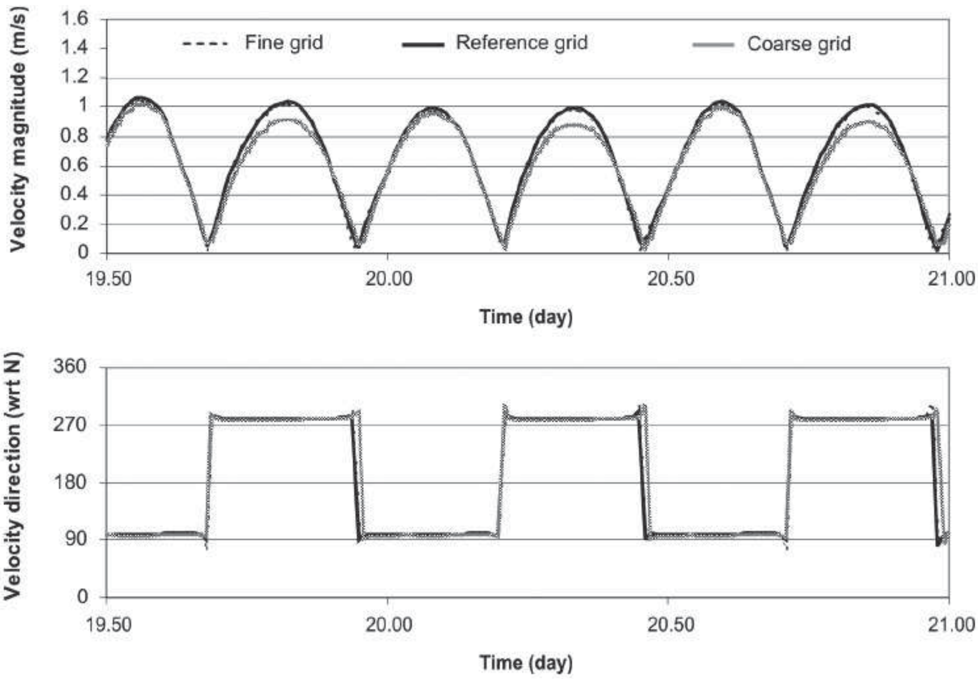

Fig. 6: Dependency of velocity variability on grid resolution in cross-section 7 – position 2 (Fig. 4)

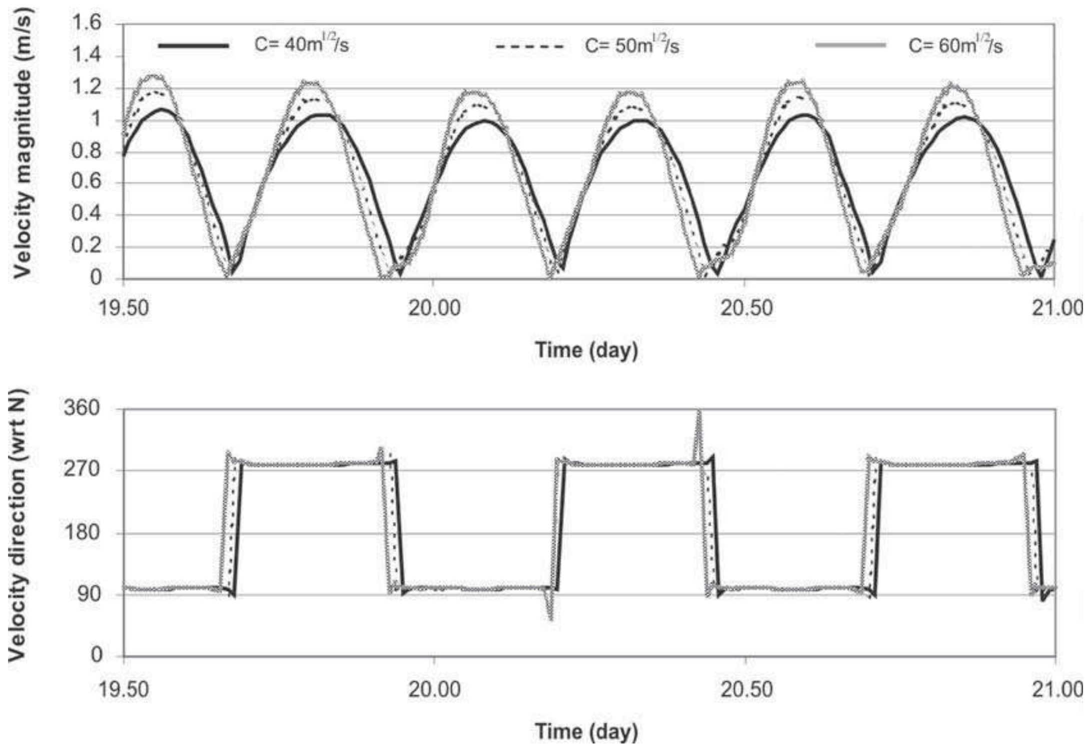

Fig. 7: Dependency of velocity variability on bottom roughness in cross-section 7 – position 2 (Fig. 4)

In order to compare the results obtained from a 2DH and a 3D flow model the reference grid of the 2DH model was extended to include 10 layers in the vertical direction. The vertical grid size distribution of the 3D model was chosen to follow a logarithmic distribution in order to accurately reproduce the vertical flow profile. Comparisons between the 2DH and 3D flow model computations were made for water levels at several locations and

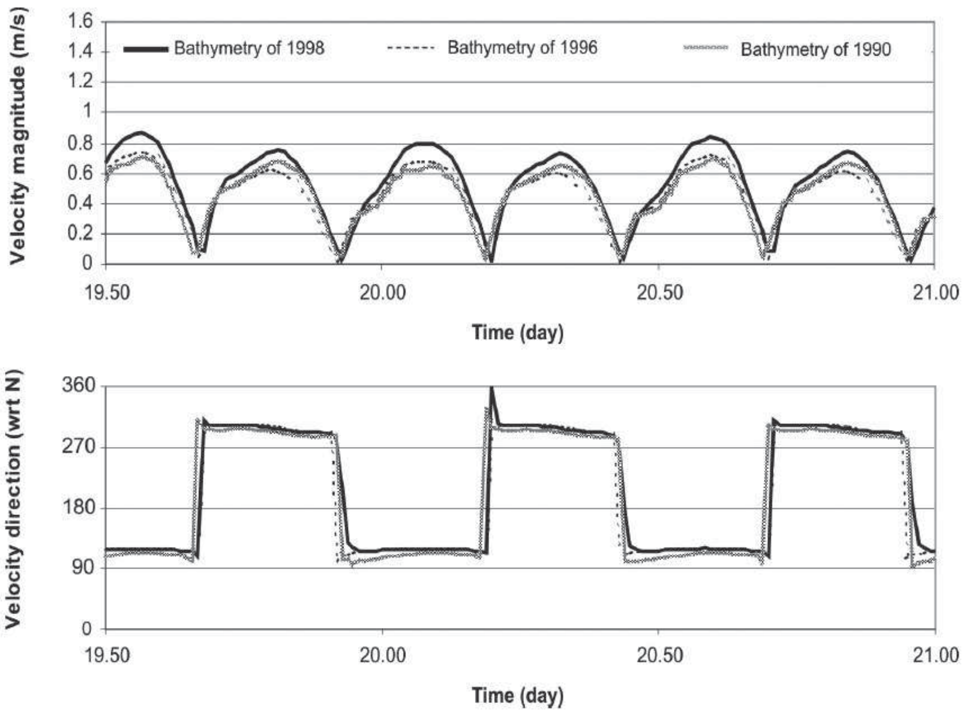

Fig. 8: Dependency of velocity variability on bathymetry in cross-section 8 – position 1 (Fig. 4)

current velocities in a number of cross-sections. A comparison between the depth-averaged current velocities computed by the 2DH model and those obtained by depth-averaging the results of the 3D model runs is shown by way of example during maximum ebb flow over the cross-section at the intersection of Suederpiep and Norderpiep tidal channels in Fig. 9. It was found that the results given by the two flow models are fairly similar during most of the tidal period, except during slack water, when current reversal occurs.

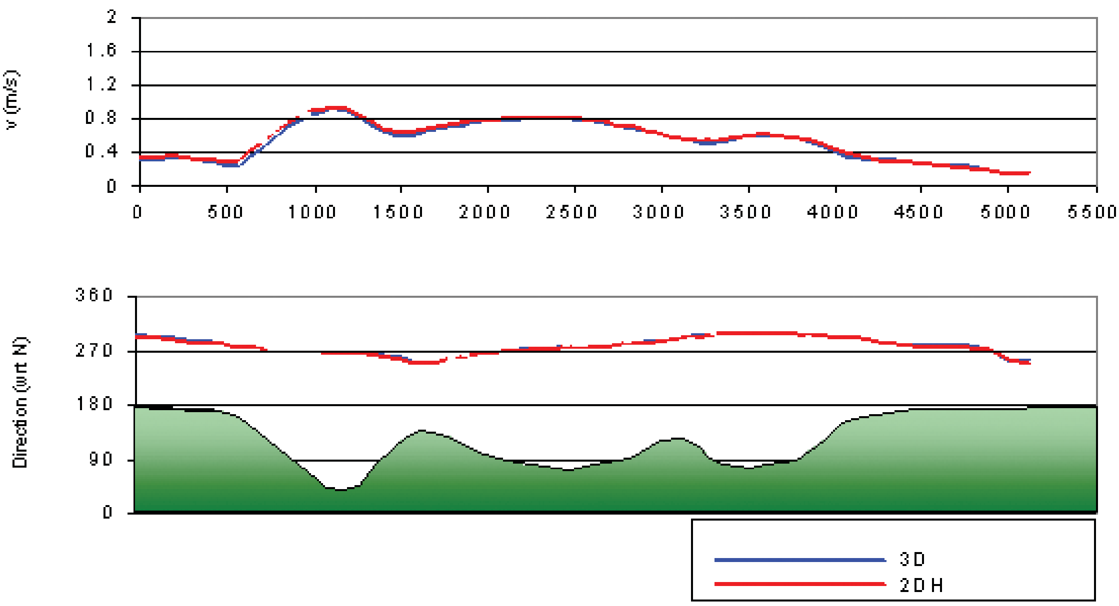

Fig. 9: Comparison between measured depth-averaged current velocities and the results obtained from 2DH and 3D model simulations during maximum ebb flow

Based on the results of the sensitivity tests presented in the foregoing, the following main model settings were chosen: a) a time step of 0.5 min; b) a constant spatial and temporal eddy viscosity value of 1 m²/s; c) a curvilinear grid with a grid spacing ranging between 60 and 180 m. Furthermore, the sensitivity tests indicated that the flow field in the study area is mainly governed by the forcing conditions imposed on the open sea boundary, and to a lesser extent by bathymetry and the selected value of bed roughness. These parameters were taken into consideration in the calibration process presented in the following section. In order to avoid the effects of initial conditions on the computational results a sufficiently long warming-up period (of about 48 hours) was included in all simulations.

Fig. 10 shows the resulting variation of depth-integrated current velocities over a tidal period computed using the above-mentioned models settings. The results indicate that the model is capable of realistically reproducing the main flow patterns, with current velocities directed onshore and offshore during the flood and ebb phases, respectively, and a tendency towards zero current velocities at high and low water slack. Based on visual observations, drying and flooding of the sandbanks are also reproduced well by the model.

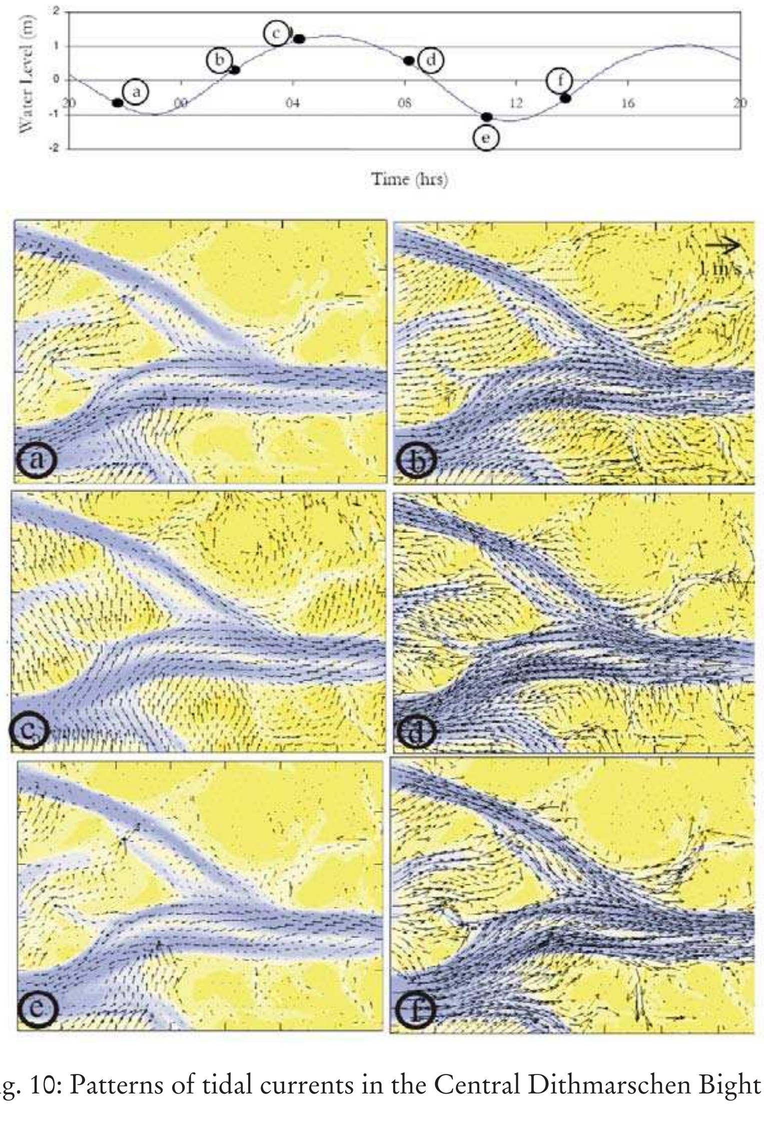

Fig. 10: Patterns of tidal currents in the Central Dithmarschen Bight

5. Calibration and Validation Data

Calibration and validation of the flow model were carried out using measured water levels and current velocities covering the full range of conditions typical of the study area. Complete sets of data were compiled for driving the model and evaluating its performance. These include wind velocity fields covering the modelled area and water levels near the open sea boundaries for driving the flow model as well as water levels measured at a number of locations and current velocities measured over several cross-sections for calibration and validation purposes. The selected sets of measured data are listed in Table 2.

Water levels measured over six periods (P_{N1} to P_{N6}) covering entire lunar cycles were used for calibrating and validating the model with respect to surface elevation. The astronomical tidal range varied from about 2.3 m to 4.2 m from neap to spring tides, respectively. The predictive capability of the model with regard to surface elevations during harsher meteorological conditions was also tested for three periods (P_{S1} to P_{S3}) incorporating storms with water level set-ups and wind velocities of up to about 4.5 m and 33 m/s, respectively.

The data measured at the following gauge stations were used for model calibration and validation: G1: Blauort; G2: Tertius; G3: Trischen; G4: Buesum, G5: Steertloch and G6: Flackstrom. The locations of these gauge stations are shown in Fig. 1. Stations G1 to G3 are located along the western boundary of the investigation area at the entrances to the Norderpiep and Suederpiep tidal channels, station G4 is located near Buesum harbour, and stations G5 and G6 are situated fairly close to the coastline.

Table 2: Observation periods considered for model calibration and validation

Periods			Duration	Characteristics	Gauges/ Transects
Calibration	Water levels	P_{N1}	May 31–Jun 26/1989	Relatively calm weather conditions	G1 to G6
		P_{N2}	May 31–Jul 12/1990		
		P_{N3}	Apr 27–Jun 30/1990		
	Current Velocities	P_{V4}	Jun 5–6/2000		T1 to T3
		P_{V3}	Sep 12–13/2000		
Validation	Water levels	P_{N4}	Jul 7–Aug 18/1990	Relatively calm weather conditions	G1 to G6
		P_{N5}	Aug 15–Sep 15/2000		
		P_{N6}	Sep 22–Oct 22/2000		
		P_{S1}	Jan 25–31/1990	Storm periods with wind speeds of up to 33 m/s and water level set-ups of up to 4.5 m	
		P_{S2}	Feb 25–Mar 1/1990		
		P_{S3}	Nov 26–Dec 5/1999		
	Current Velocities	P_{V5}	Mar 21–23/2000	Relatively calm weather conditions	T1 to T3
		P_{V2}	Sep 5–6/2000		
		P_{V1}	Dec 5–6/2000		

Flow measurements over several cross-sections in the tidal channels served as a basis for calibrating and validating the model with respect to current velocities. The cross-sections surveyed by moving vessels are shown in Fig. 1. These measurements were made under relatively calm weather conditions using a 1200 kHz Acoustic Doppler Current Profiler (ADCP) manufactured by RD Instruments. Details of the measurement procedure as well as the results of an analysis to determine the spatial and temporal variations of current velocity in the tidal channels are given in TORO et al. (in this volume).

Five relatively calm periods (P_{V1} to P_{V5}) covering tidal ranges varying from about 2 m to 4 m were selected for calibrating and validating the model with respect to current velocities. During the calibration and validation procedures, attention was focused on the ability of the model to reproduce current velocities in three cross-sections, i.e. T1 and T2 at the entrance to the central Dithmarschen Bight in the Norderpiep and Suederpiep tidal channels, respectively, and T3 in the Piep tidal channel nearer to the coast. The bed profiles of these cross-sections are shown in Fig. 1. Further details of the selected cross-sections and the procedure adopted for determining depth-averaged current velocities are given in TORO et al. (in this volume).

6. Assessment of Model Performance

The predictive capability of the flow model with regard to water levels and current velocities was verified by comparing measured and modelled values. A set of statistical parameters was used to assess the quality of the model results. In this study the Mean Error (ME), the Mean Absolute Error (MAE), the Relative Mean Absolute Error (RMAE) and the Adjusted Relative Mean Absolute Error (ARMAE) were used for assessment purposes. Definitions of these parameters are listed in Table 3. The ME serves to indicate a general tendency of predictions towards overestimation or underestimation. The standard deviation of the differences between predicted and observed values is a measure of the variability of the differences about the mean value of the differences. As a dimensional parameter, it indicates quite clearly the magnitude of the error and hence the accuracy of a simulation. Division of the MAE by the mean absolute value of the measurements yields the non-dimensional RMAE.

WALSTRA et al. (2001) and VAN RIJN et al. (2002) have proposed a set of standards for assessing model performance in connection with model studies of two coastal areas (see Table 4). The severity of these standards depends on the complexity of the environmental conditions at the location concerned. It should be noted that the measurements used to check model performance in the latter cases were made at fixed locations in both coastal areas. The viability of applying such standards to measurements from moving vessels with a much wider spatial and temporal coverage (as in the present investigation) should thus be borne in mind. As measurements always include errors, a suggested approach to account for the influence of observational errors is to subtract these from each absolute error, thereby yielding an Adjusted Relative Mean Absolute Error (ARMAE). In the present study the accuracy of water level measurements at the gauge stations was taken to be 1 cm. Based on an investigation by JIMENEZ-GONZÁLEZ et al. (in this volume) of the accuracy of acoustic profiling measurements from moving vessels, it was deduced that the accuracy of depth-averaged current profiles over the cross-sections of the tidal channels surveyed in the present study was about 0.015 m/s.

7. Model Calibration

The model calibration procedure involved the adjustment of physical parameters so as to obtain the best possible reproduction of hydrodynamic conditions in the study area. The periods selected for model calibration in the present investigation (see Table 2) were chosen to cover a wide range of conditions typical of the modelled domain. Calibration with respect to water levels was carried out for three periods characterized by relatively calm weather conditions. The predictive capability of the model with regard to current velocities (as defined in Section 6) was investigated for two relatively calm periods, i.e. June 5 to 6, 2000 and September 12 to 13, 2000 with tidal ranges of 3.9 m and 3.3 m, respectively.

Simulations were performed for the three model domains shown in Fig. 2. Comparable results were obtained in each case. Only the results obtained from the Extended Central Dithmarschen Bight Model (ECDBM) using measured water levels along the open sea boundaries are presented in the following. The wind field obtained from the PRISMA interpolation model was applied in all simulations (LUTHARDT, 1987).

Calibration of the flow model was carried out in two steps. In the first step, hydrodynamic forcing along the open sea boundary was adjusted to improve the predictive capability of the model with respect to water levels. For this purpose measured and computed water levels were compared at a number of locations. In the second step, the bed roughness in the tidal channels was adjusted so as to obtain the best possible agreement between measured and computed current velocities. Although the bathymetry of the study area was also found to influence current velocities, it was not possible to quantify this effect in detail due to a lack of adequate bathymetric measurements covering the entire domain for periods corresponding to the dates of the measuring campaigns.

Table 3: Statistical parameters used for model calibration and validation

Parameter	Equation
Mean Error	$ME = \sum_{j=1}^{n} (Mod_j - Mea_j) / n$ (1)
Mean Absolute Error	$MAE = \sum_{j=1}^{n} \mid (Mod_j - Mea_j) \mid / n$ (2)
Relative Mean Absolute Error	$RMAE = \sum_{j=1}^{n} \left(\mid Mod_j - Mea_j \mid \right) / \sum_{j=1}^{n} \mid Mea_j \mid$ (3)
Adjusted Relative Mean Absolute Error	$ARMAE = \sum_{j=1}^{n} \left(\mid Mod_j - Mea_j \mid Ac \right) / \sum_{j=1}^{n} \mid Mea_j \mid$ (4)

Note: Mod= Model results; Mea=Measured values;
n= Number of values; Ac= Accuracy of measurements

Table 4: Performance rating according to the RMAE of velocity values

Rating	RMAE VAN RIJN et al. (2002)	RMAE WALSTRA et al. (2001)
Excellent	< 0.1	< 0.2
Good	0.1–0.3	0.2–0.4
Reasonable / Fair	0.3–0.5	0.4–0.7
Poor	0.5–0.7	0.7–1.0
Bad	> 0.7	> 1.0

7.1 Hydrodynamic Forcing along the Open Sea Boundaries

As the computed water levels in the study area were found to depend primarily on the conditions specified along the western open sea boundary, the performance of several approaches for prescribing hydrodynamic forcing in terms of water levels was investigated. The results of a detailed investigation of the effects of hydrodynamic forcing along the open sea boundaries of coastal models are presented by MAYERLE et al. (in this volume(b)). The effectiveness of several approaches was tested for a wide range of conditions covering periods of up to two months. These include approaches based on measured water levels at gauge stations located close to the model open sea boundaries and the use of simulated water levels obtained from a larger-scale model covering the adjacent sea area. The results obtained by specifying water levels along the open sea boundaries of the ECDBM are presented in this study. Due to the fact that water levels specified along the western open sea boundary of the flow model were obtained from gauge stations located some 10 km further eastwards within the model domain (stations G1 to G3 in Fig. 1), appropriate corrections to the measured water levels were necessary. Satisfactory predictions were obtained by reducing the amplitudes and phases of the measured water levels by about 5 % and 15 min, respectively.

The statistical parameters obtained at the six gauge stations G1 to G6 are listed in Table 5. Fig. 12 and 13 show the resulting mean errors (ME) and mean absolute errors (MAE) with the corresponding standard deviations for high and low water amplitudes and phases, respectively. The results indicate that the MAE of amplitudes and phases are generally less than about 10 cm and 20 cm, and 15 min and 25 min at high and low water, respectively.

7.2 Bed Roughness

The effect of bed roughness on model predictions of current velocities was assessed according to the procedure outlined in Section 6. For this purpose a comparison was made between measured and modelled current velocities at cross-sections T1 in the Norderpiep, T2 in the Suederpiep and T3 in the Piep tidal channel based on simulations covering two two-day periods (June 5 to 6, 2000 and September 12 to 13, 2000).

The simulations were initially performed using Chézy coefficients ranging between 50 and 65 $m^{1/2}/s$. On the basis of these simulations it was found that a Chézy coefficient of about 60 $m^{1/2}/s$ yielded the best agreement between modelled and measured current velocities. Fig. 11a shows the corresponding equivalent roughness sizes. Further simulations were then performed with bed roughness under additional consideration of geological features and bed-form dimensions (see Fig. 11b). Comparisons between the results obtained using the two maps of bed roughness shown in Fig. 11 indicate that although there is a certain reduction in the magnitudes and changes in the patterns of depth-averaged current velocities due to a higher bed roughness at certain locations, only minor changes resulted in the statistical parameters obtained for the entire analysis period (see Table 6). The depth-averaged current velocities computed in the channels using the two roughness maps showed little difference owing to their large water depths. The most pronounced differences in the magnitudes and patterns of depth-averaged current velocities due to a higher bed roughness were observed at cross-sections T2 and T3. With regard to currents, the main effect of higher bed roughness values is to delay the time of occurrence of peak velocities. Investigations carried out by MAYERLE et al. (in this volume (a)) have shown that bed roughness has a much greater effect on sediment concentrations. This stresses the importance of describing bed roughness as accurately as possible in order to adequately reproduce the patterns of sediment dynamics and associated morphological developments.

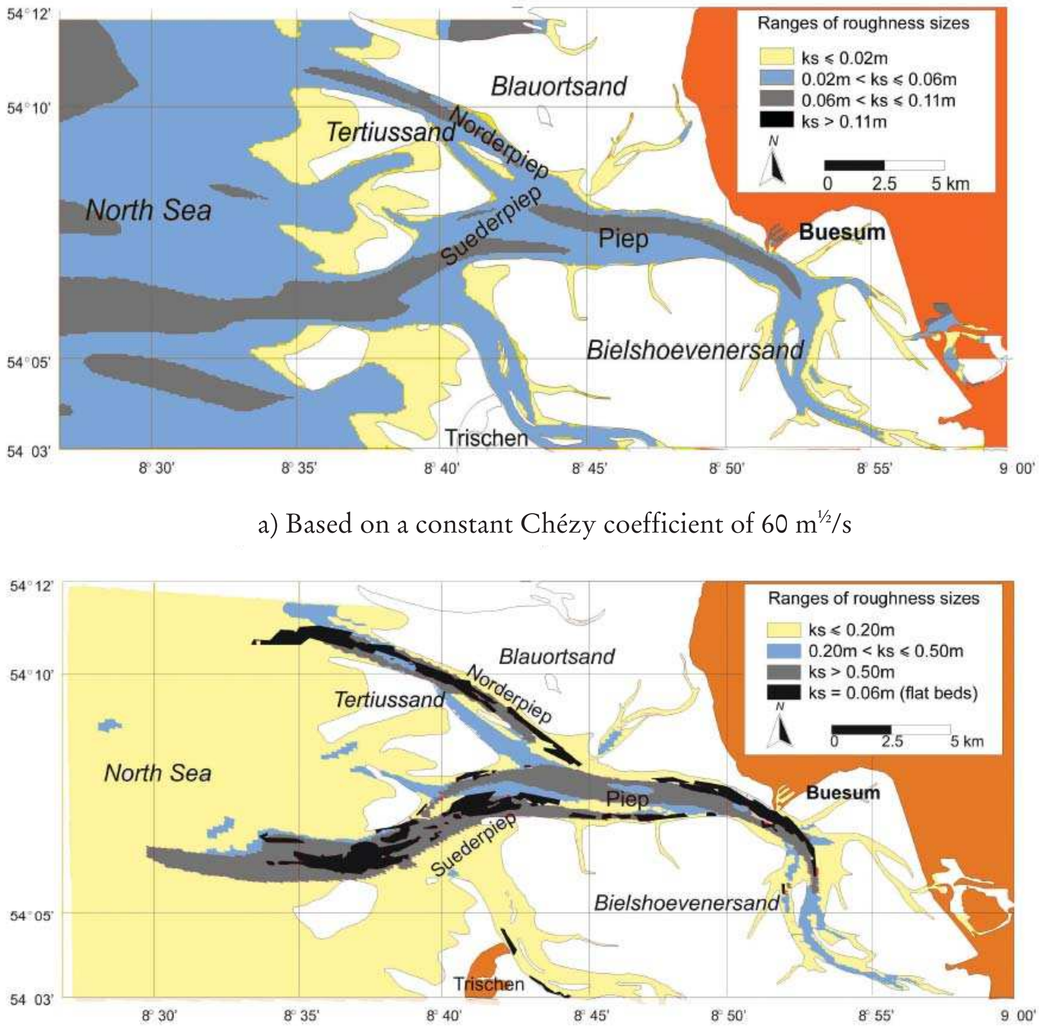

a) Based on a constant Chézy coefficient of 60 $m^{½}/s$

b) Accounting for geological features and bed-form dimensions

Fig. 11: Maps of equivalent roughness sizes (MAYERLE et al., this volume (a))

Table 6 lists the statistical parameters obtained from a comparison of measured and computed current velocities in the main tidal channels. The mean errors (ME), mean absolute errors (MAE), and corresponding standard deviations between measured and computed values of high and low water amplitudes, phases (gauge stations G1 and G5), and depth-averaged current velocities (cross-sections T1 to T3) are shown in Figs. 12, 13 and 18, respectively. On the basis of the ME values the model shows a certain tendency to underestimate the magnitude of current velocities, particularly at cross-section T1. The MAE of depth-averaged current velocities is found to vary between 0.10 m/s and 0.30 m/s, with ARMAE values ranging between 0.09 and 0.27. For the conditions investigated, slightly better agreement was obtained at cross-section T3 nearer the coast.

8. Model Validation

The ability of the model to correctly reproduce field conditions was assessed in the validation procedure by comparing the results of model simulations with measured data. The numerical and physical parameters defined for model set-up, sensitivity studies and calibration were held constant throughout the entire validation process. As in the calibration procedure, all model runs were performed using water levels along the open sea boundaries based on measurements at nearby gauge stations and wind fields generated by the PRISMA model. Although the data sets used for model validation differed from those used for model calibration (see Table 2), the same gauge stations (G1 to G6) and cross-sections (T1 to T3) were used for validating water levels and current velocities, respectively. Model validation with respect to water levels included three relatively calm periods (P_{N4} to P_{N6} in Table 2) and three periods with storms (P_{S1} to P_{S3} in Table 2). The predictive capability of the model with regard to current velocities (see Section 6) was verified for three relatively calm periods during the year 2000, i.e. March 21 to 23, September 5 to 6, and December 5 to 6. Similar to the approach adopted in the calibration procedure, the water levels measured at gauge station G2 were suitably adjusted to obtain representative values along the western open sea boundary.

The model validation results for water levels and current velocities are listed in Table 5 and 6, respectively. The mean errors (ME), mean absolute errors (MAE), and corresponding standard deviations between measured and computed values of high and low water amplitudes and phases (gauge stations G1 and G5) are shown in Fig. 12 and 13, respectively.

The ME values for water levels indicate a tendency towards overestimation of high water levels and underestimation of low water levels. The corresponding MAE values are found to generally lie below 10 cm and 20 cm for high and low water levels, respectively, representing about 3 % to 6 % of the mean tidal range. With regard to tidal phase, the computed times of high and low water were found to lag measurements. A time lag of between 10 and 20 min (1.5 % to 3 % of the tidal period) and 10–30 min (1.5 % to 4 % of the tidal period) were obtained at high and low water levels, respectively. As would be expected, better agreement is obtained at the gauge stations located closer to the western open sea boundary.

Fig. 14 and 15 show comparisons of measured and computed water levels at gauge stations G1 to G6 for the period August 4 to August 18, 2000 (period P_{N4}). The results presented in the figures cover about two weeks of the simulated periods. It is seen that fairly good agreement is obtained between observations and model predictions at all gauge stations, with only minor discrepancies confined mainly to low water conditions. The ability of the model to handle extreme events was also investigated. Comparisons of measured and computed water levels obtained from simulations covering several storms are shown in Fig. 16 and 17. As may be seen in the figures, the model is able to simulate extreme events fairly well, with discrepancies generally less than about 30 cm at high water.

Fig. 18 shows ME and MAE values with corresponding standard deviations between measured and computed values of depth-averaged current velocities at cross-sections T1 to T3 (see Fig. 1). The MAE for depth-averaged current velocities was found to range between 0.12 m/s and 0.22 m/s for the majority of cross-sections and observation periods, which represents about 10 % to 20 % of tidally-averaged values. Agreement between model results and observations was found to be much better for neap tides than for spring tides. Better agreement was obtained at cross-section T3 located nearer the coast and at cross-section T2, through which most of the tidal discharge is transported into and out of the domain. At cross-section T1 the model tends to underestimate depth-averaged current velocities. The ARMAE values were found to lie below 0.2 for the majority of measurement conditions and cross-sections. According to the standards proposed by WALSTRA et al. (2001) and VAN RIJN et al. (2002), the performance of the model is classified as being excellent, and between good and excellent, respectively. It should be noted that the discrepancies between model predictions and observations are partly attributable to a lack of bathymetric measurements close to the periods during which measurements were made over the surveyed cross-sections. The fact that measurements were performed from moving vessels as well as the application of an extrapolation procedure to describe velocity profiles over the entire depth are also potential sources of error.

Comparisons of measured and computed current velocities for a neap tide (December 5 to 6, 2000) are shown in Figs. 19 to 24. It is seen that the model is capable of reproducing current velocities over the selected cross-sections fairly well. In general, it was found that the model is unable to correctly reproduce the variation of current velocities during certain phases of the tidal cycle, particularly at slack water. This may be related to the 2DH model approximation, which appears to inadequately reproduce changes in flow direction.

Table 5: Model calibration and validation results for water levels (ECDBM)

		Gauge Station	Amplitude				Phase			
			High water level		Low water level		High water level		Low water level	
			ME (STD) in cm	MAE (STD) in cm	ME (STD) in cm	MAE (STD) in cm	ME (STD) in min	MAE (STD) in min	ME (STD) in min	MAE (STD) in min
CALIBRATION	P_{N1}	G1	5.4 (1.0)	5.4 (1.0)	–13.3 (2.5)	13.3 (2.5)	–8.1 (11.7)	11.5 (8.4)	–8.2 (13.4)	12.2 (9.8)
		G2	9.9 (1.7)	9.9 (1.7)	–8.4 (6.4)	8.4 (6.4)	–6.0 (12.3)	10.8 (8.2)	–0.7 (17.7)	12.6 (12.3)
		G3	4.4 (1.2)	4.4 (1.2)	–8.1 (2.8)	8.1 (2.8)	–7.5 (11.0)	10.4 (8.3)	–25.3 (9.7)	25.3 (9.7)
		G4	N.A.	N.A.	N.A.	N.A.	N.A.	N.A.	N.A.	N.A.
		G5	–9.6 (2.1)	9.6 (2.1)	–3.9 (3.5)	4.1 (3.3)	–5.3 (13.7)	11.7 (8.8)	13.1 (15.8)	17.4 (10.8)
		G6	7.7 (2.2)	7.7 (2.2)	–18.6 (4.5)	18.6 (4.5)	–9.1 (10.6)	11.3 (8.0)	1.0 (15.4)	11.5 (10.2)
	P_{N2}	G1	5.4 (1.0)	5.4 (1.0)	–12.8 (2.7)	12.8 (2.7)	–8.6 (12.8)	12.3 (9.2)	–7.6 (12.3)	11.3 (9.0)
		G2	9.0 (2.1)	9.0 (2.1)	–7.9 (5.1)	7.9 (5.1)	–3.8 (11.6)	9.7 (7.3)	–1.6 (15.1)	11.3 (10.0)
		G3	4.1 (1.4)	4.1 (1.4)	–8.4 (3.4)	8.4 (3.4)	–6.6 (10.3)	9.6 (7.5)	–23.2 (10.2)	23.2 (10.2)
		G4	N.A.	N.A.	N.A.	N.A.	N.A.	N.A.	N.A.	N.A.
		G5	–10.5 (2.8)	10.5 (2.8)	–3.2 (9.0)	5.1 (8.1)	–6.2 (14.2)	12.4 (9.1)	13.7 (19.7)	19.0 (14.6)
		G6	7.3 (2.2)	7.3 (2.2)	–17.9 (5.2)	18.0 (5.0)	–9.7 (10.0)	11.6 (7.8)	2.3 (14.5)	10.8 (9.8)
	P_{N3}	G1	5.2 (1.7)	5.2 (1.7)	–13.0 (2.8)	13.0 (2.8)	–8.4 (12.6)	12.0 (9.2)	–6.5 (11.6)	11.0 (7.5)
		G2	9.8 (2.8)	9.8 (2.8)	–5.2 (3.4)	5.5 (3.0)	–2.7 (16.1)	12.1 (11.0)	–7.1 (13.2)	11.5 (9.6)
		G3	6.0 (4.4)	6.7 (3.3)	–5.9 (5.0)	6.4 (4.3)	–1.3 (12.6)	9.4 (8.5)	–21.0 (14.0)	21.3 (13.5)
		G4	4.2 (6.1)	5.9 (4.4)	–27.6 (6.7)	27.6 (6.7)	5.2 (14.6)	11.7 (10.0)	9.7 (18.2)	16.0 (13.1)
		G5	4.7 (5.9)	5.8 (4.8)	–33.0 (7.3)	33.1 (7.3)	13.0 (19.4)	18.5 (14.2)	24.6 (25.2)	30.0 (18.4)
		G6	8.0 (4.8)	8.4 (4.1)	–16.7 (6.6)	16.7 (6.4)	–7.5 (13.7)	12.0 (10.0)	5.0 (10.4)	9.1 (7.1)
VALIDATION	P_{N4}	G1	0.2 (2.0)	1.5 (1.2)	–7.3 (3.4)	7.3 (3.4)	–16.5 (16.9)	19.6 (13.1)	–7.3 (3.4)	10.4 (9.7)
		G2	6.0 (2.7)	6.2 (2.3)	1.5 (3.5)	3.2 (2.0)	–11.6 (16.1)	15.6 (12.2)	2.7 (13.5)	11.3 (7.8)
		G3	3.1 (0.8)	3.1 (0.8)	–2.6 (1.5)	2.6 (1.5)	–12.4 (11.9)	13.7 (10.4)	–11.0 (14.4)	13.7 (11.8)
		G4	4.1 (3.7)	4.2 (3.5)	–6.1 (3.4)	6.2 (3.3)	–1.1 (14.2)	11.2 (8.8)	13.3 (13.4)	16.1 (9.8)
		G5	3.7 (7.3)	5.3 (6.2)	–10.4 (4.7)	10.5 (4.6)	5.0 (22.0)	16.0 (15.4)	21.8 (18.8)	24.2 (15.5)
		G6	5.5 (2.8)	5.6 (2.7)	–1.6 (3.8)	3.4 (2.3)	–14.0 (13.4)	15.8 (11.2)	10.6 (13.5)	14.4 (9.3)
	P_{N5}	G1	4.6 (1.2)	4.6 (1.2)	–8.8 (2.9)	8.8 (2.9)	–0.4 (14.5)	12.0 (7.9)	–3.0 (13.5)	10.8 (8.4)
		G2	0.0 (1.4)	1.0 (0.9)	–11.2 (2.9)	11.2 (2.9)	1.0 (9.6)	7.5 (5.9)	–5.4 (10.3)	8.2 (8.2)
		G3	5.1 (1.6)	5.1 (1.6)	–2.8 (3.7)	4.0 (2.3)	–4.9 (8.9)	7.7 (6.6)	–18.1 (10.6)	18.1 (10.6)
		G4	5.3 (3.0)	5.3 (3.0)	–18.5 (5.2)	18.5 (5.2)	10.4 (10.1)	11.4 (8.9)	9.9 (22.8)	21.1 (13.0)
		G5	1.9 (5.1)	4.3 (3.2)	–21.9 (6.9)	21.9 (6.9)	6.3 (11.9)	10.2 (8.7)	10.8 (33.6)	31.9 (14.5)
		G6	N.A.	N.A.	N.A.	N.A.	N.A.	N.A.	N.A.	N.A.
	P_{N6}	G1	4.6 (1.3)	4.6 (1.3)	–7.2 (3.4)	7.3 (3.2)	–2.3 (16.3)	13.6 (9.0)	–8.9 (11.9)	12.1 (8.6)
		G2	–0.1 (2.0)	1.6 (1.2)	–9.6 (3.8)	9.6 (3.8)	0.9 (13.1)	9.6 (8.9)	–7.4 (12.6)	11.6 (8.7)
		G3	5.5 (1.9)	5.5 (1.9)	–1.5 (3.1)	2.8 (2.0)	–3.3 (8.2)	6.7 (5.8)	–16.8 (13.2)	17.5 (12.3)
		G4	5.3 (2.3)	5.3 (2.3)	–12.0 (4.5)	12.0 (4.5)	12.3 (12.9)	13.7 (11.4)	–2.1 (35.9)	29.3 (19.3)
		G5	6.6 (3.9)	6.7 (3.7)	–17.6 (8.3)	17.8 (8.0)	9.8 (13.3)	12.2 (11.1)	0.3 (36.1)	31.3 (17.5)
		G6	N.A.	N.A.	N.A.	N.A.	N.A.	N.A.	N.A.	N.A.

where: NA: values not available

Table 6: Model calibration and validation results for current velocities (ECDBM)

Period		Range of WL and (V)	Cross-Sections (No. of transects)	Bed roughness based on a constant Chézy coefficient of 60 $m^{0.5}/s$			Bed roughness considering geological features and bed-form dimensions		
				ME (STD) in m/s	MAE (STD) in m/s	ARMAE	ME (STD) in m/s	MAE (STD) in m/s	ARMAE
CALIBRATION	P_{V4}	3.7 to 3.9 (1.4 to 1.7)	T1 (15)	–0.29 (0.17)	0.30 (0.16)	0.27	–0.27 (0.17)	0.28 (0.16)	0.25
			T2 (13)	–0.09 (0.21)	0.18 (0.14)	0.19	–0.09 (0.22)	0.19 (0.14)	0.2
			T3 (9)	0.04 (0.20)	0.17 (0.11)	0.18	–0.04 (0.21)	0.18 (0.11)	0.19
	P_{V3}	3.3 to 3.5 (1.3 to 1.6)	T1 (28)	–0.13 (0.16)	0.17 (0.13)	0.17	–0.15 (0.18)	0.18 (0.14)	0.19
			T2 (7)	–0.04 (0.24)	0.20 (0.15)	0.21	–0.05 (0.26)	0.21 (0.15)	0.24
			T3 (6)	–0.06 (0.11)	0.10 (0.08)	0.09	–0.11 (0.15)	0.16 (0.11)	0.17
VALIDATION	P_{V5}	4.0 to 4.2 (1.4 to 1.6)	T1 (18)	–0.04 (0.19)	0.16 (0.11)	0.15	–0.08 (0.2)	0.18 (0.12)	0.18
			T2 (6)	0.09 (0.25)	0.22 (0.15)	0.34	0.06 (0.24)	0.20 (0.14)	0.32
			T3 (16)	0.04 (0.16)	0.13 (0.09)	0.14	–0.01 (0.16)	0.13 (0.10)	0.13
	P_{V2}	2.9 to 3.2 (0.9 to 1.3)	T1 (20)	–0.15 (0.20)	0.20 (0.14)	0.22	–0.14 (0.21)	0.20 (0.16)	0.22
			T2 (10)	–0.05 (0.19)	0.15 (0.12)	0.18	–0.06 (0.19)	0.16 (0.12)	0.2
			T3 (7)	–0.07 (0.13)	0.12 (0.09)	0.11	–0.11 (0.11)	0.13 (0.08)	0.12
	P_{V1}	2.3 to 2.5 (0.6 to 1.1)	T1 (35)	–0.11 (0.12)	0.14 (0.09)	0.19	–0.12 (0.12)	0.14 (0.10)	0.19
			T2 (12)	–0.05 (0.14)	0.12 (0.09)	0.16	–0.06 (0.14)	0.13 (0.09)	0.17
			T3 (17)	–0.07 (0.15)	0.13 (0.10)	0.21	–0.07 (0.14)	0.12 (0.09)	0.18

where:
WL: Water level (m)
V: Current velocity (m/s)
STD: Standard deviation

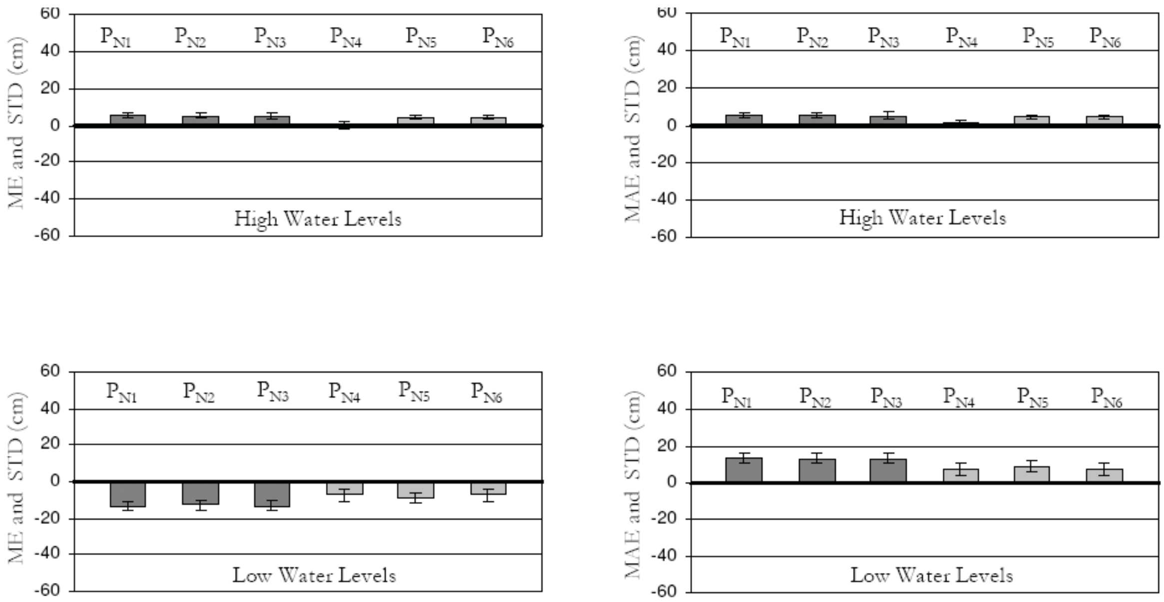

a) Gauge Station 1

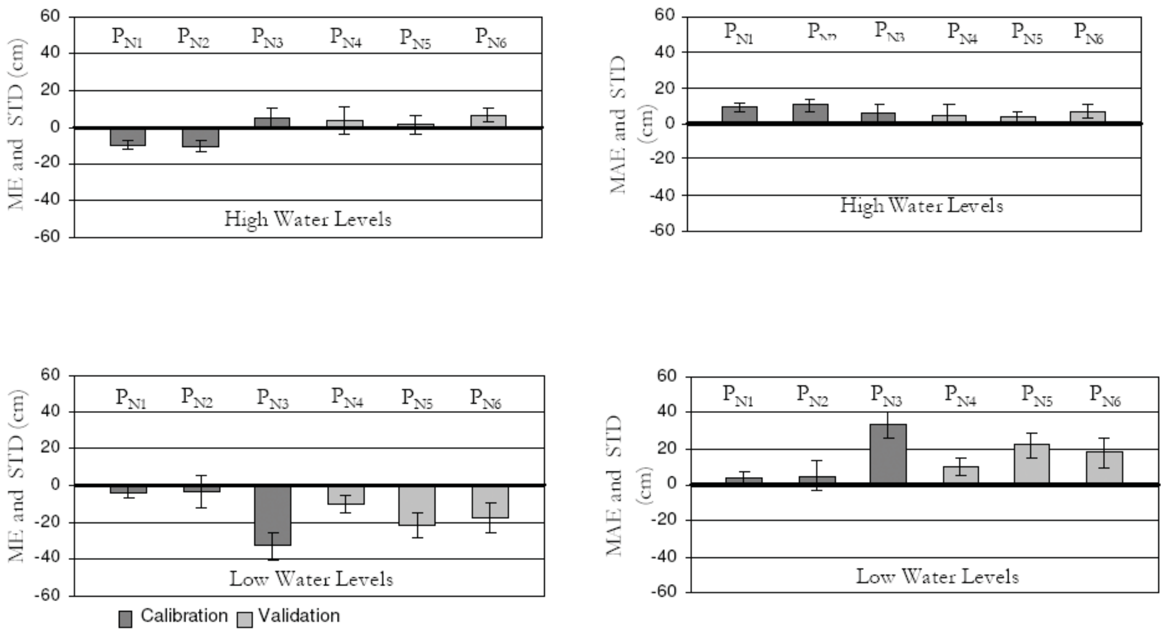

b) Gauge Station 5

Fig. 12: Mean Error (ME), Mean Absolute Error (MAE), and corresponding standard deviations of amplitudes at high and low water levels (gauge stations G1 and G5)

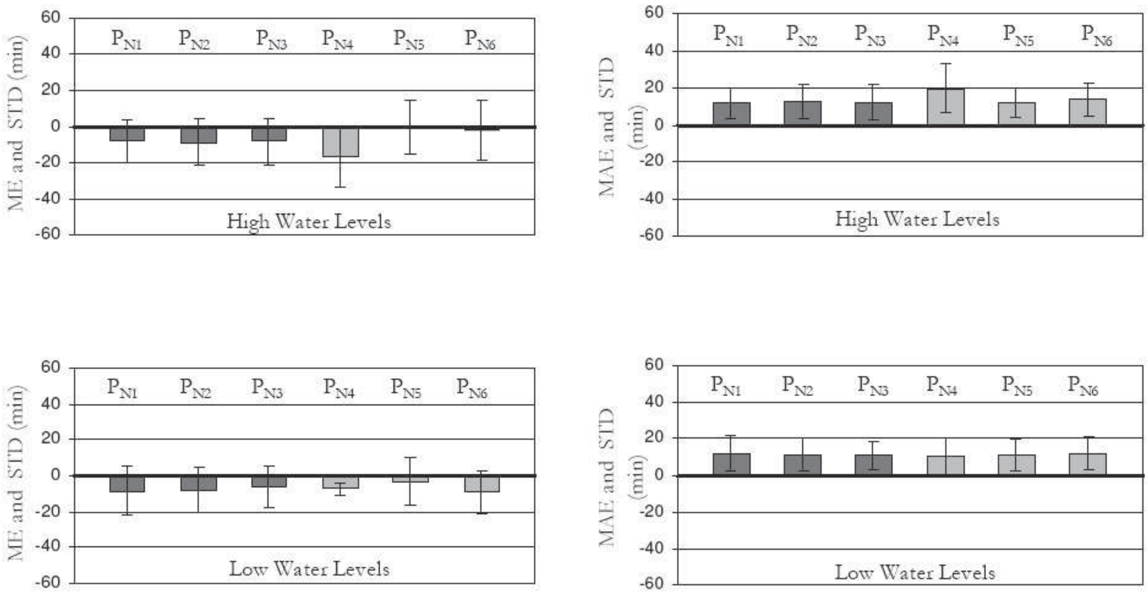

a) Gauge Station 1

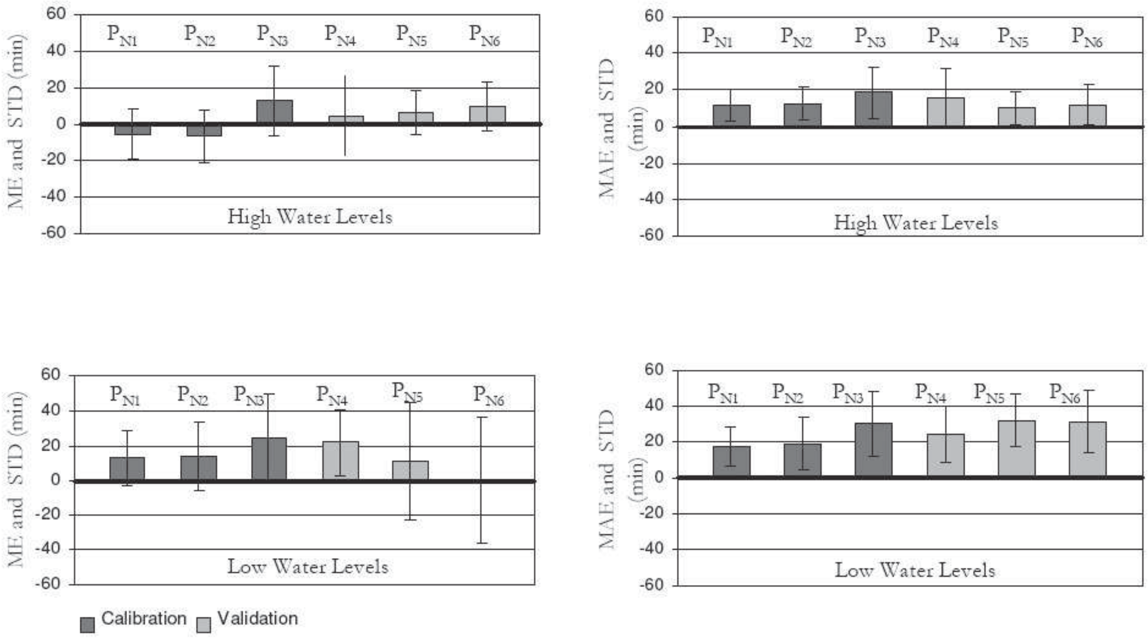

b) Gauge Station 5

Fig. 13: Mean Error (ME), Mean Absolute Error (MAE), and corresponding standard deviations of phases at high and low water levels (gauge stations G1 and G5)

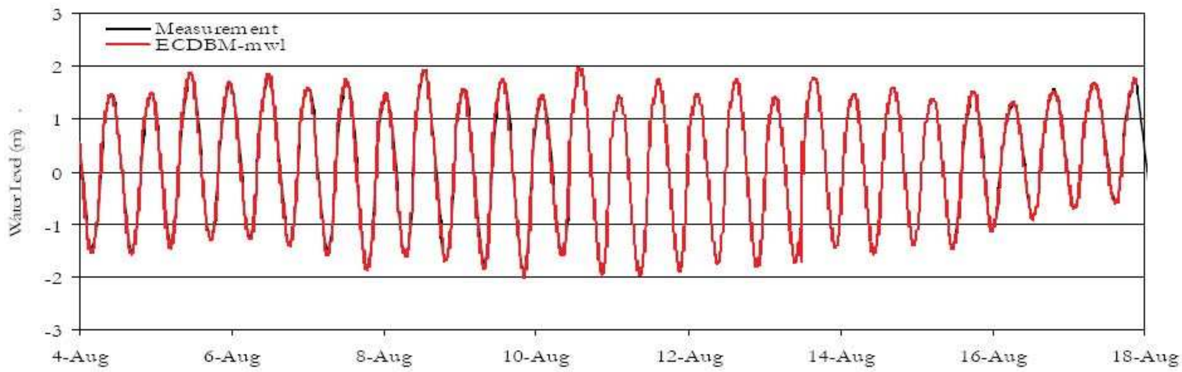

a) Gauge Station G1 (Blauort)

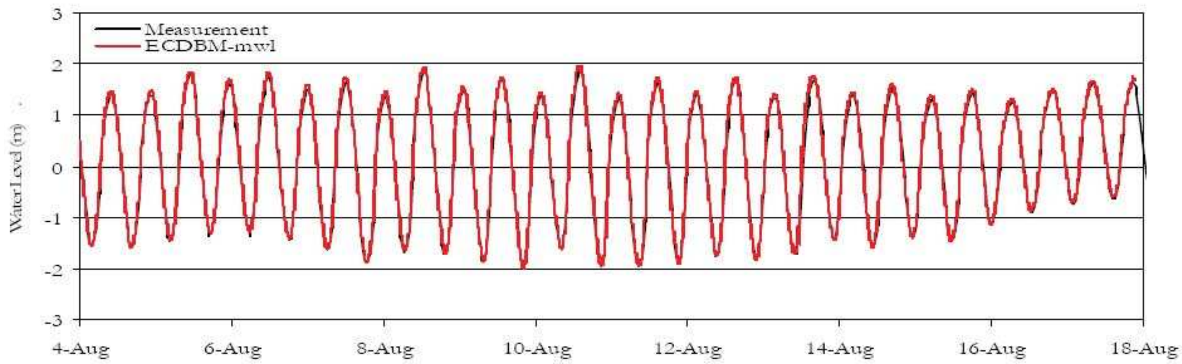

b) Gauge Station G2 (Tertius)

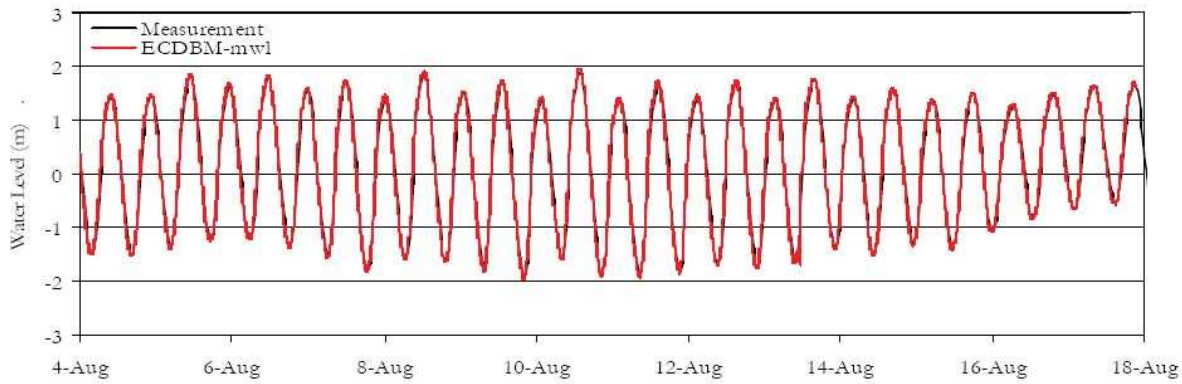

c) Gauge Station G3 (Trischen)

Fig. 14: Comparisons between measured and computed water levels at gauge stations G1 to G3 for observation period P_{N4}

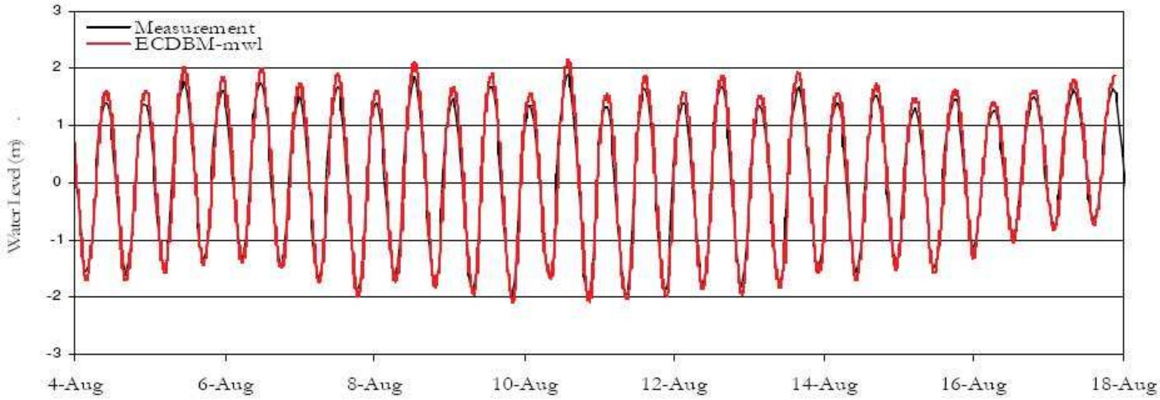

a) Gauge Station G4 (Buesum)

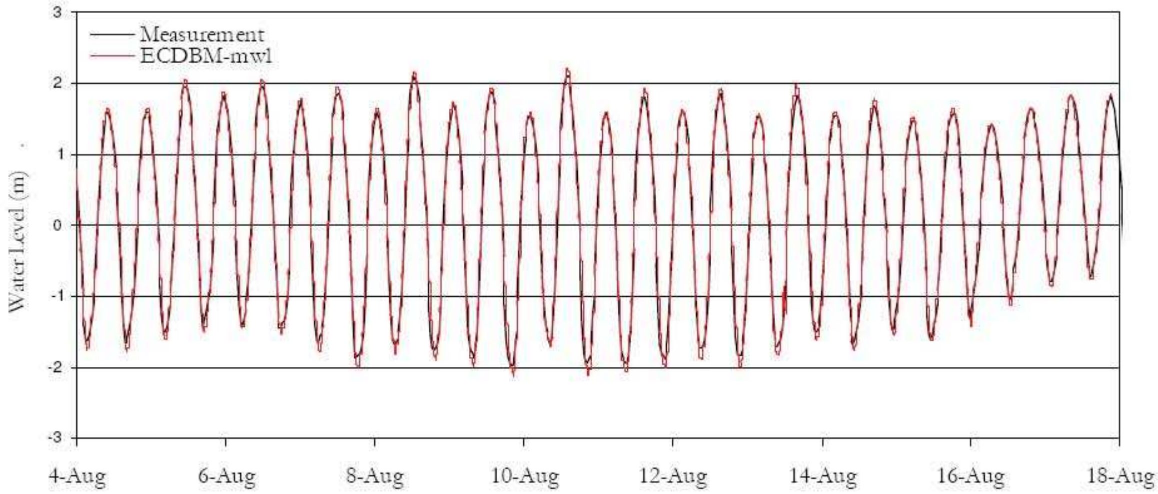

b) Gauge Station G5 (Steertloch)

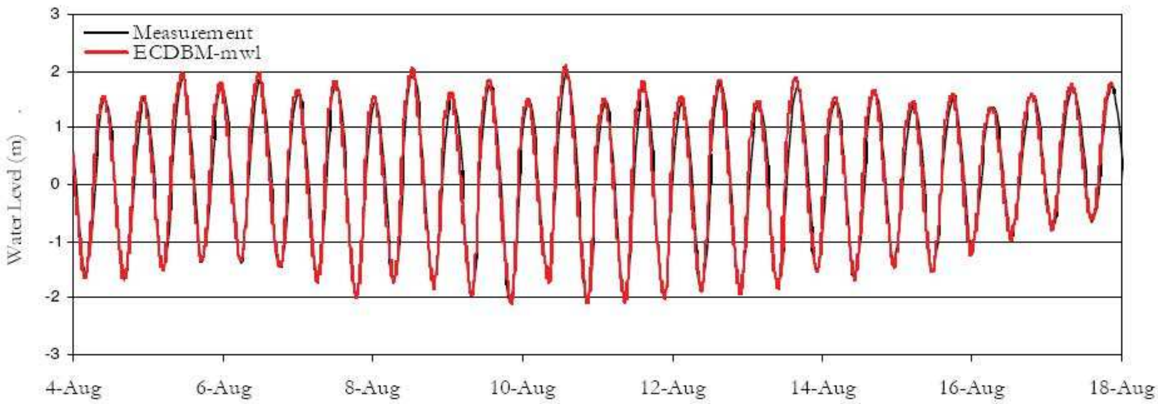

c) Gauge Station G6 (Flackstrom)

Fig. 15: Comparisons between measured and computed water levels at gauge stations G4 to G6 for observation period P_{N4}

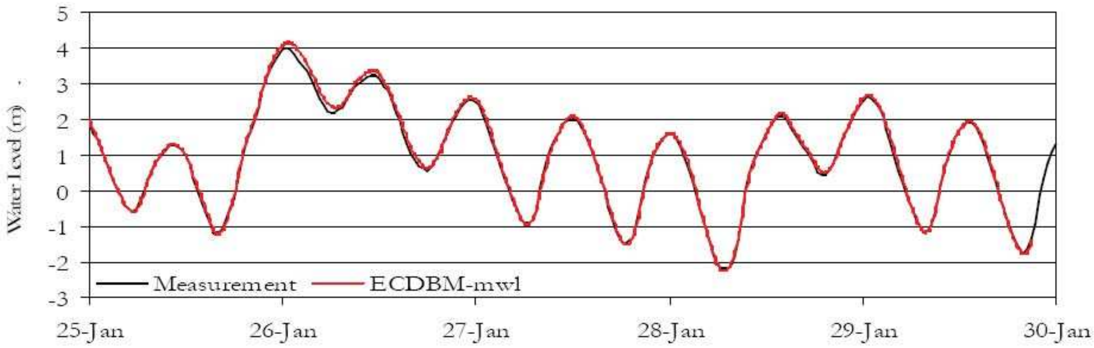

a) Period P_{S1}: Jan 25 to 31, 1990

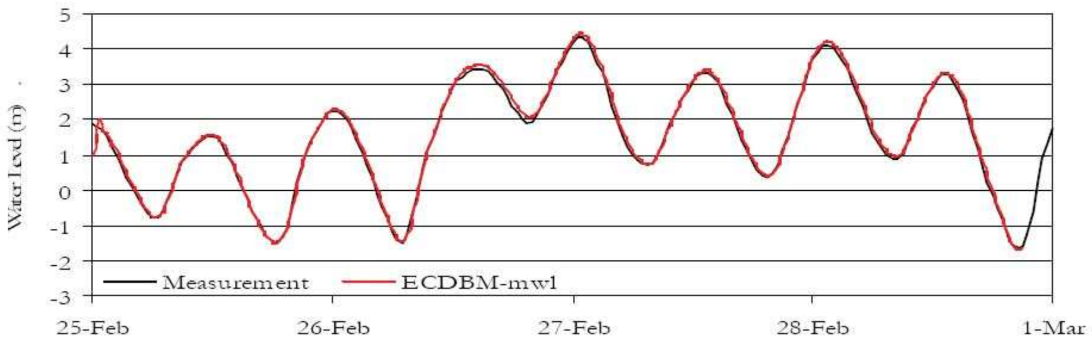

b) Period P_{S2}: February 25 to March 1, 1990

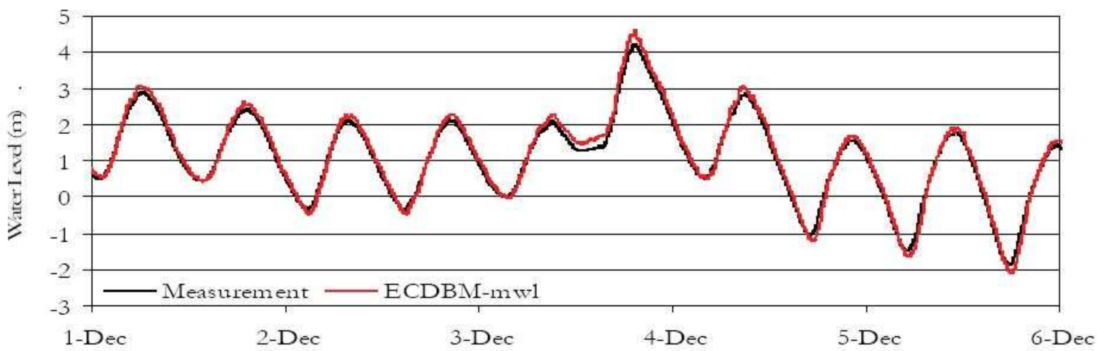

c) Period P_{S3}: December 1 to 6, 1999

Fig. 16: Comparisons between measured and computed water levels during storm periods at gauge station G1 (Blauort)

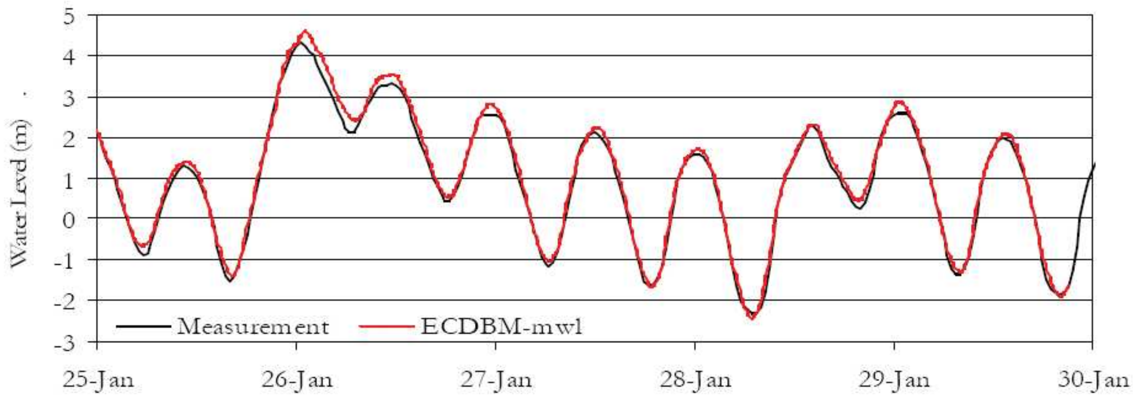

a) Period P_{S1}: Jan 25 to 31, 1990

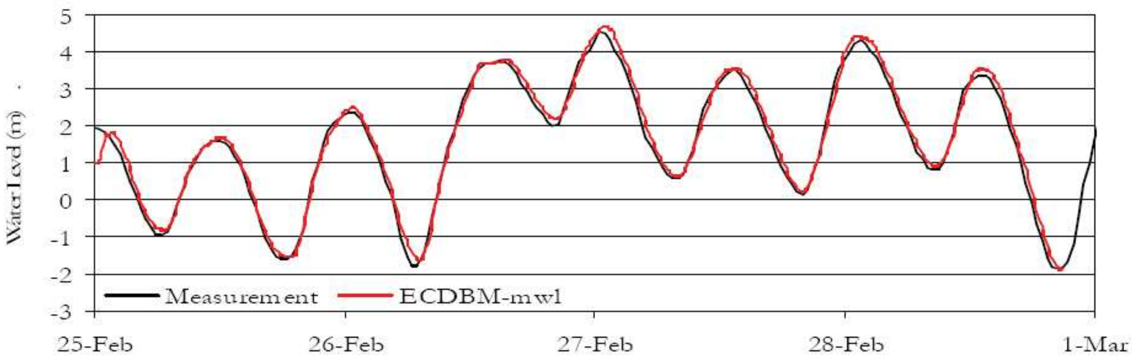

b) Period P_{S2}: February 25 to March 1, 1990

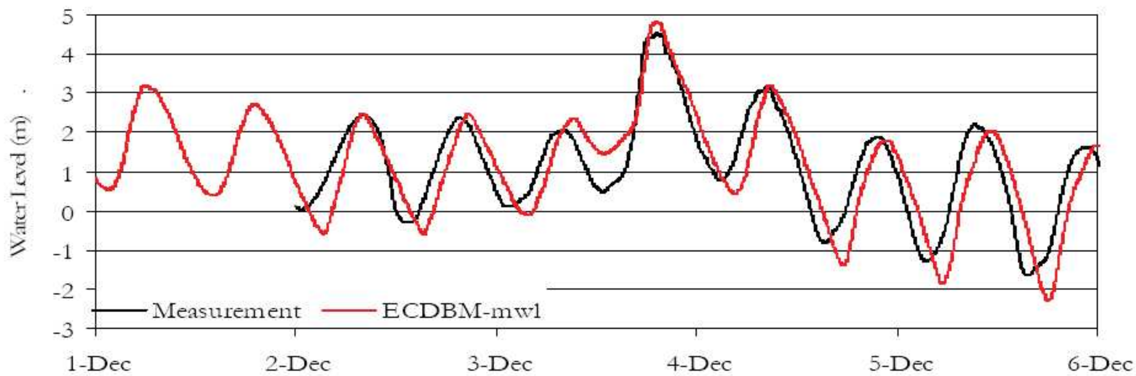

c) Period P_{S3}: Dec 1 to 6, 1999

Fig. 17: Comparisons between measured and computed water levels during storm periods at gauge station G4 (Buesum)

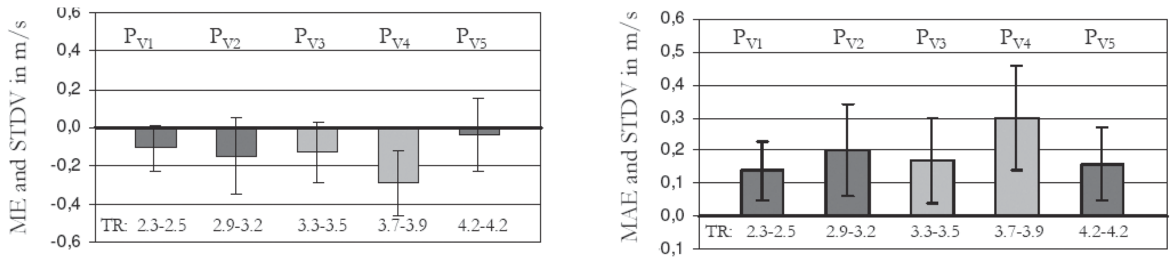

a) Cross-section T1

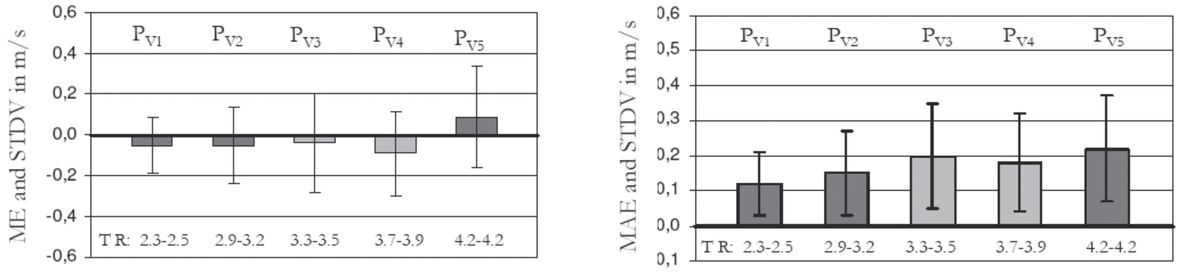

b) Cross-section T2

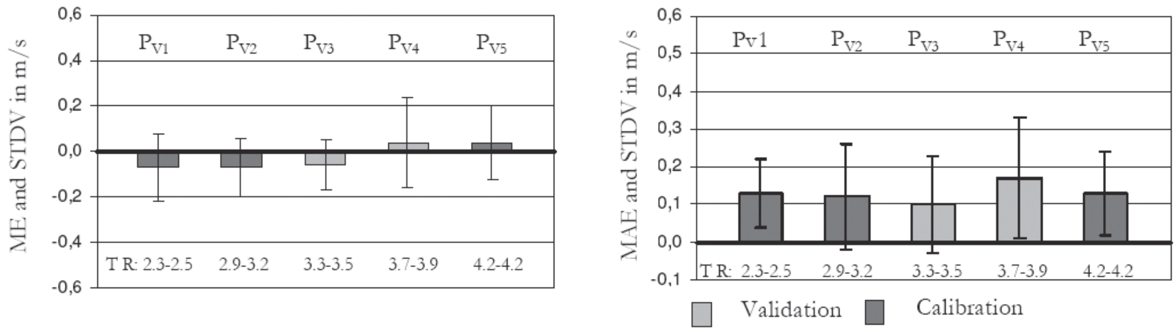

c) Cross-section T3

Fig. 18: Mean error (ME), Mean Absolute Error (MAE), and corresponding standard deviations of depth-averaged current velocities at cross-sections T1 to T3 for observation periods P_{V1} to P_{V5} shown in Table 2

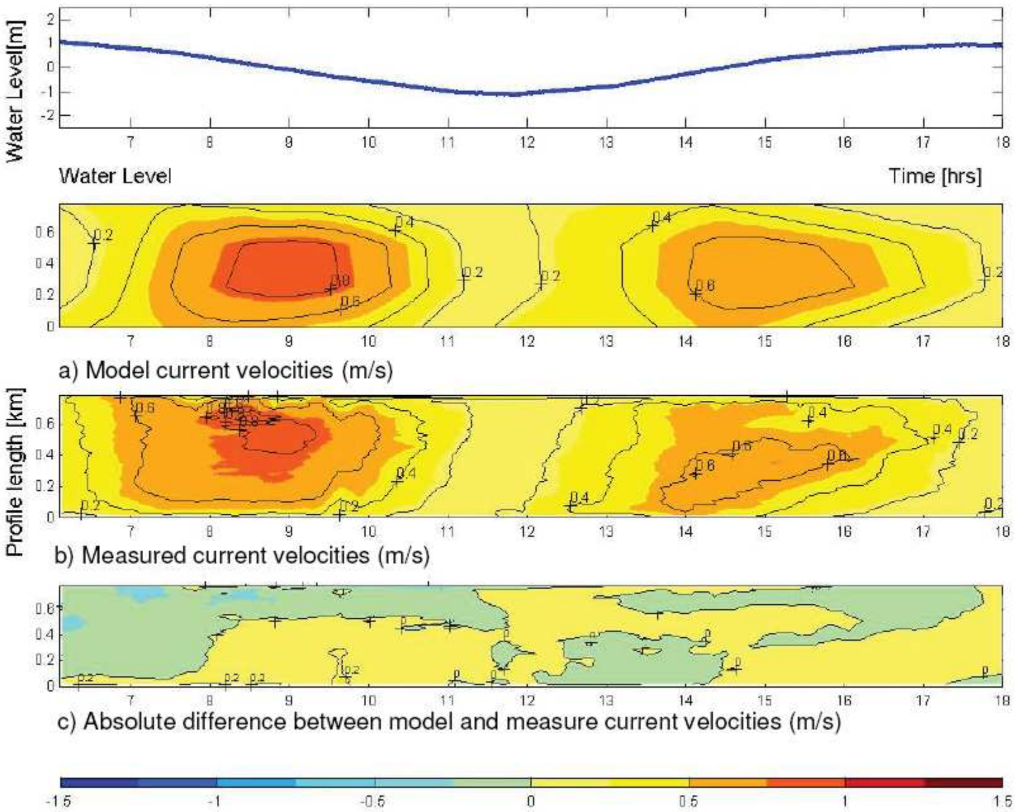

Fig. 19: Measured versus computed variation in depth-averaged current velocity at cross-section T1 on December 5, 2000

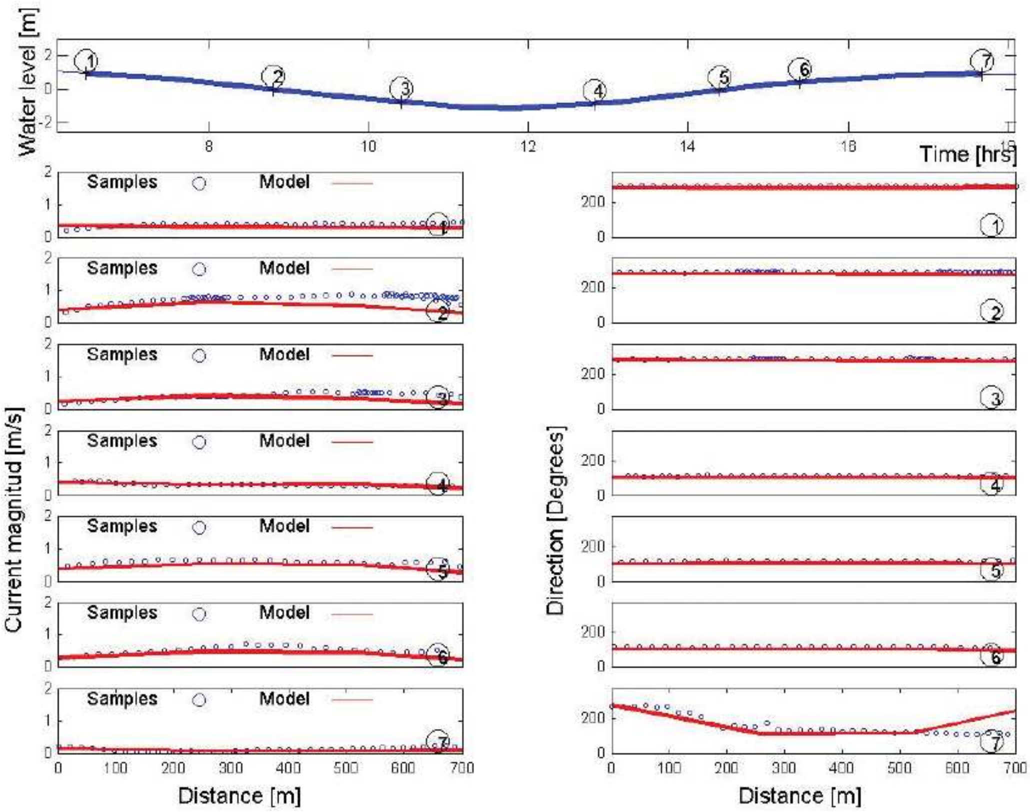

Fig. 20: Measured versus computed variation of cross-sectional distribution of current velocity at cross-section T1 on December 5, 2000

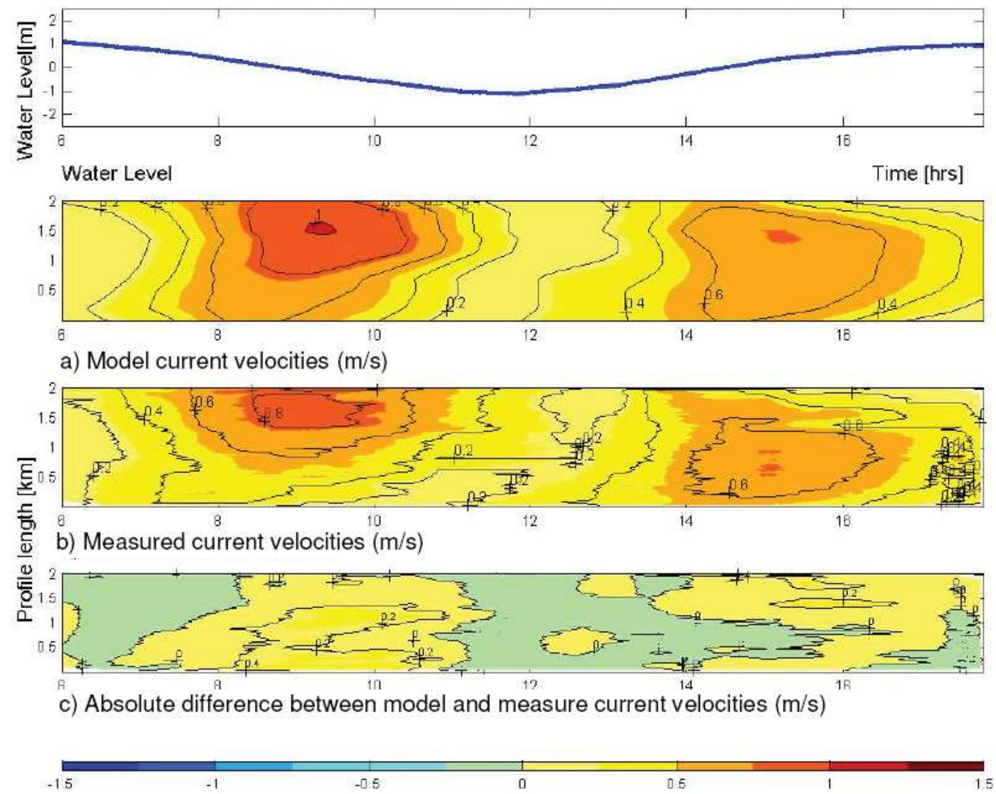

Fig. 21: Measured versus computed variation in depth-averaged current velocity at cross-section T2 on December 5, 2000

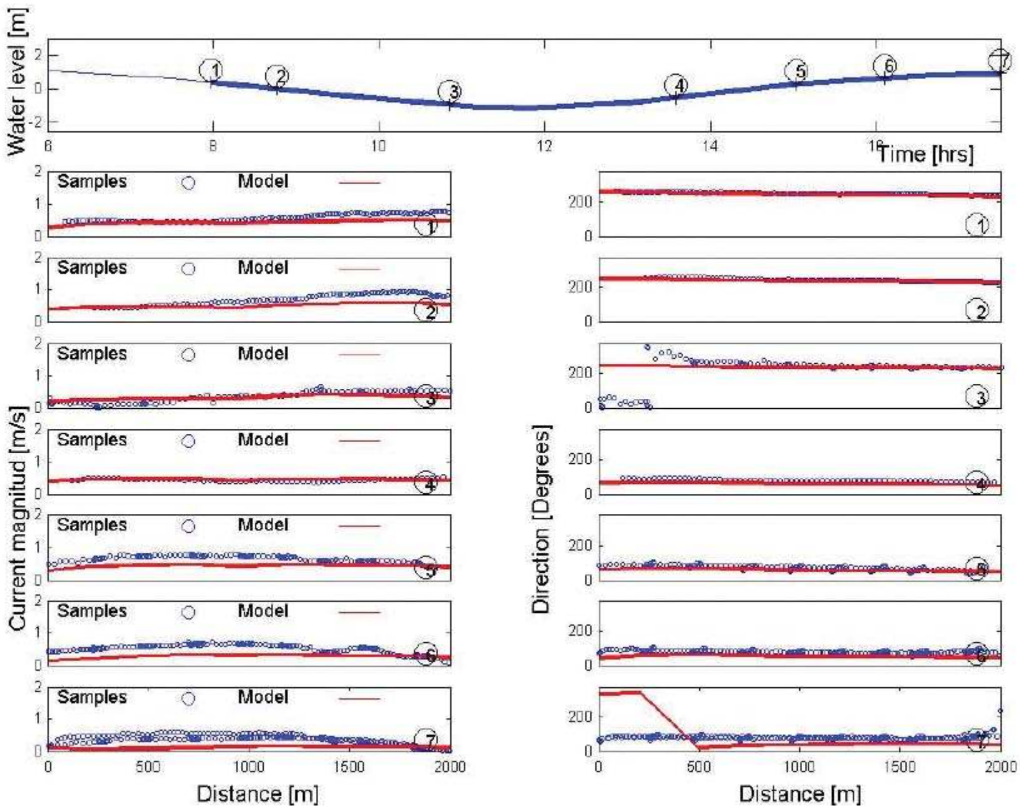

Fig. 22: Measured versus computed variation of cross-sectional distribution of current velocity at cross-section T2 on December 5, 2000

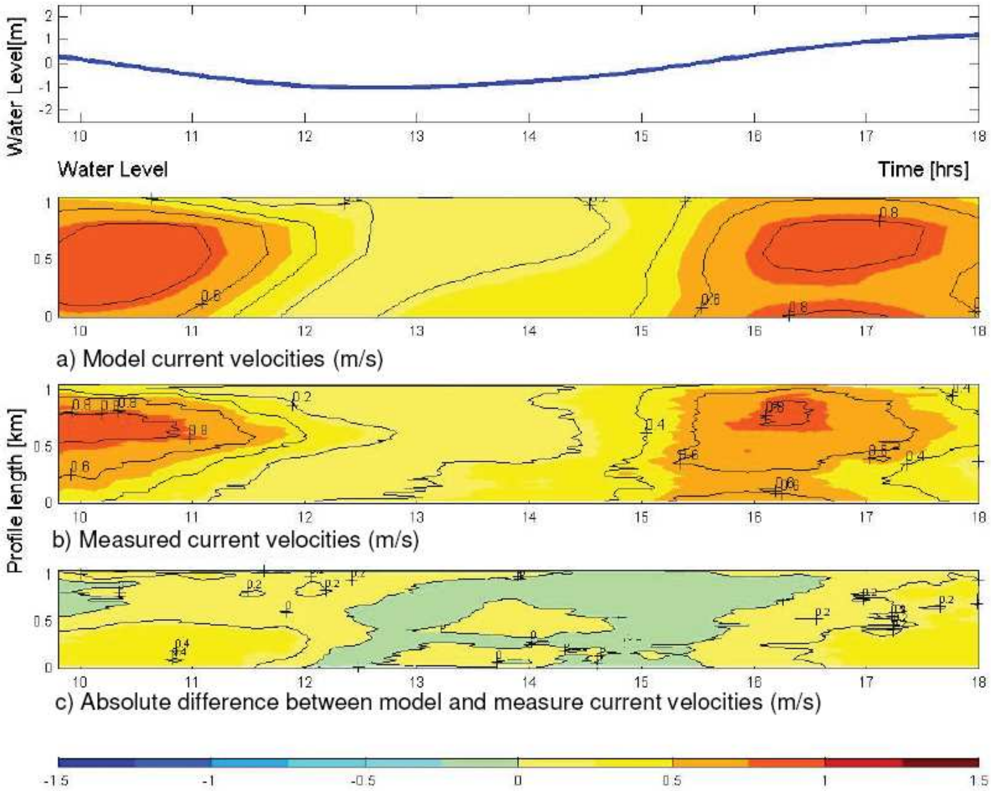

Fig. 23: Measured versus computed variation in depth-averaged current velocity at cross-section T3 on December 6, 2000

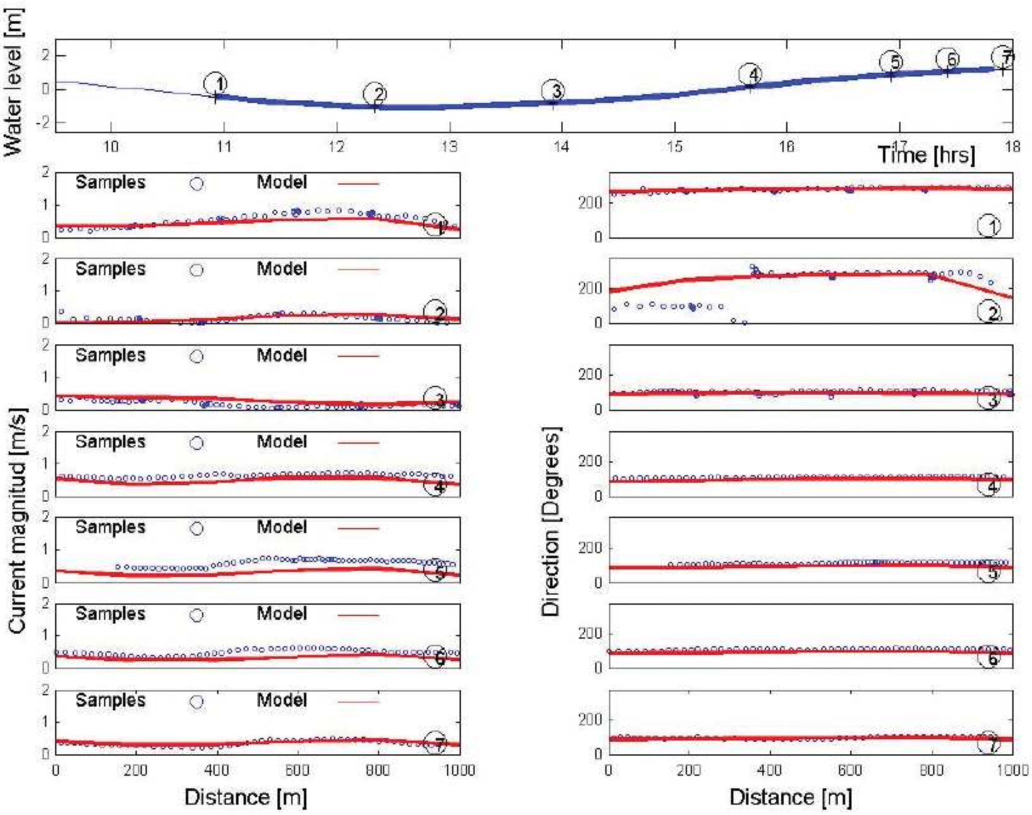

Fig. 24: Measured versus computed variation of cross-sectional distribution of current velocity at cross-section T3 on December 6, 2000

9. Conclusions

- This paper describes the development stages of a flow model for the central Dithmarschen Bight. The flow model was developed in several steps, including model set-up, sensitivity studies, and model calibration and validation. A two-dimensional depth-integrated flow approximation based on the DELFT3D Modelling System developed by Delft Hydraulics in the Netherlands was implemented in the study.
- Three flow models covering areas ranging from 300 km² to 1640 km² were set-up. The models implement curvilinear grid systems adjusted to the bathymetry derived from measurements made in 1998. Bathymetric maps prepared in 1990 were employed for modelling the tidal flat regions of the study area. In the model simulations water levels were imposed along the open sea boundaries and wind data were specified at the grid nodes using the PRISMA wind interpolation model developed at the Max Planck Institute of Meteorology in Hamburg (LUTHARDT, 1987). Flow discharges were specified along the open boundaries at the mouths of the Eider and Elbe estuaries.
- Sensitivity studies were carried out in order to assess the relative influence of the main physical and numerical model parameters on computed water levels and current velocities at various locations and cross-sections in the modelled domain. The optimum settings were determined. The sensitivity studies also revealed that wind speeds below 8 m/s have almost no effect on local water levels or depth-averaged current velocities. By comparing the results of simulations with and without the effect of waves it was found that although the effect of waves on currents is negligible in the tidal channels, this can be appreciable on the sandbanks. The relevance of three-dimensional flow model approximations was also investigated. A comparison between depth-averaged velocity distributions (2DH model) and averaged three-dimensional velocity profiles over the vertical (3D model) yielded similar results during the flood and ebb phases. The most pronounced differences between the simulation results occur at slack water, particularly during current reversal.
- A central aspect of the investigation concerns model calibration and validation based on extensive field measurements. In addition to water level recordings at several gauge stations covering several months, selective measurements of current velocities over a number of cross-sections in the main tidal channels covering the entire range of tidal conditions were employed for this purpose. Based on the quality standards normally adopted (WALSTRA et al., 2001; VAN RIJN et al., 2002), the performance of the model with regard to current velocity predictions was estimated to lie between excellent and good. In view of the fact that these assessments are still in their infancy, further work is necessary to arrive at generally acceptable standards.
- It was found that the predictive capability of the flow model mainly depends on the hydrodynamic forcing specified along the open sea boundaries. More detailed investigations of the effects of hydrodynamic forcing along the open sea boundaries of coastal models are presented in MAYERLE et al. (in this volume(b)). All of the approaches considered yield good predictions regarding water levels and current velocities. Slightly better agreement was obtained by specifying water levels measured at gauge stations along the open sea boundaries. In view of the latter, this approach was subsequently adopted throughout this study.
- The influence of bathymetry on water levels and particularly current velocities is also significant, bearing in mind that seasonal variations in seabed levels may be as much as 3 to 5 m. A certain percentage of the observed discrepancies is thus attributable to a dynamically changing bathymetry, which is not accounted for in the model.

- Investigations were also carried out to assess the effects of varying bed roughness on flow conditions in the modelled domain. It was found that relatively small equivalent roughness sizes corresponding to Chézy coefficients of about 60 $m^{1/2}/s$ yielded the best agreement between measured and computed current velocities. Although the effects of bed roughness were found to have a minor influence on the overall flow field, investigations by MAYERLE et al. (in this volume(a)) have shown that bed roughness may have a significant effect on sediment transport. It was found that the spatial variation of bed-form dimensions and associated roughness values are highly dependent on the layer thickness of potentially mobile sediments, the characteristics of superficial seabed sediments, and local flow conditions. In view of the fact that spatial variations in bed roughness may significantly affect bed shear stresses and hence sediment transport rates, it is important to take account of the latter in the flow model.
- Verification of the performance of the model for simulating water levels and current velocities was carried out for a wide range of conditions typical of the study area. The results showed that the flow model is capable of reproducing water levels and current velocities in the study area in fair agreement with observations. In general, the mean absolute error in terms of water levels at various locations over a period of several months was found to lie below 10 cm and 20 cm at high and low water levels, respectively. This corresponds to less than about 3 % to 6 % of the mean tidal range. The mean absolute error in terms of depth-averaged current velocities in several cross-sections of the tidal channels for a wide range of conditions generally ranged between 0.12–0.22 m/s, corresponding to about 10 % to 20 % of the tidally-averaged value. In this respect, better agreement was obtained for smaller tidal ranges. As bed-form dimensions are directly related to tidal range, improvements in the predictive capability of the model may be achieved by adjusting the bed roughness accordingly.

10. Acknowledgements

The results presented in this paper form a contribution to the research project "Predictions of Medium-Scale Morphodynamics – PROMORPH". We would like to thank the German Ministry of Education and Research (BMBF) for funding the project (Funding number 03 F 0262A). Funds provided by COLCIENCIAS in Colombia to finance the doctorate studies of Dr. Carlos Palacio are also highly appreciated. We are also grateful to the staff of the Research and Technology Centre "Westcoast" of the University of Kiel for carrying out the field measurements. The Regional Office for Rural Areas (ALR) in Husum is acknowledged for kindly providing the water level data and bathymetric data for the tidal flat areas. We also wish to thank the Federal Maritime and Hydrographic Agency (BSH) in Hamburg for providing the bathymetric data in the tidal channels as well as the Max Planck Institute of Meteorology in Hamburg for providing the PRISMA model data. We are also indebted to Dr. Ian Westwood for his meticulous corrections and final proofreading of the English manuscript. The constructive comments by Dr.-Ing. V. Barthel and an anonymous reviewer are also gratefully acknowledged.

11. References

ASP NETO, N. E.: Long- to Short-term Morphodynamic Evolution of the Tidal Channels and Flats of the Dithmarschen Bight, German North Sea, Ph.D. thesis, University of Kiel, Germany, 2004.

HARTSUIKER, G.: Deutsche Bucht and Dithmarschen Bucht, Set-up and Calibration of Tidal Flow Models. Delft, Delft Hydraulics, Report H1821, 1997.

HIRSCHHÄUSER, T. and ZANKE, U.: Morphologische Langfristprognose für das System Tidebecken-Außenände am Beispeil Sylts und der Dithmarscher Bucht, Die Küste, Heft 64, 2001, pp 127–160.

JIMÉNEZ-GONZÁLEZ, S.; MAYERLE, R. and EGOZCUE, J. J.: A Proposed Approach for Determination of the Accuracy of Acoustic Profilers for Field Conditions, Die Küste, Heft 69, 2005.

LUTHARDT, H.: Analysis of pressure and wind fields along the Nord Sea on the basis of routine observations (in German) Hamburger Geophysikalische Einzelschriften, Reihe A 83. Department of Geosciences, University of Hamburg, Germany, 109 pp., 1987.

MAYERLE, R.; PRAMONO, G. and ESCOBAR, C. A.: Dimension and Roughness Distribution of Bed Forms in Tidal Channels in the German Bight, Die Küste, Heft 69, 2005 (a).

MAYERLE, R.; WILKENS, J.; ESCOBAR, C. A. and WINDUPRANATA, W.: Hydrodynamic Forcing Along the Open Sea Boundaries of Small-Scale Coastal Models, Die Küste, Heft 69, 2005 (b).

PALACIO, C. A.; MAYERLE, R. and TORO, F. M.: Sensitivity analysis for the Meldorf Bight Hydrodynamic Model. XXX International Association of Hydraulic Engineering and Research Congress, Thessaloniki, Greece, August 2003.

POERBANDONO and MAYERLE, R.: Composition and Dynamics of Sediments in Tidal Channels of the German North Sea Coast, Die Küste, Heft 69, 2005 (a).

RICKLEFS, K. and ASP NETO, N. E.: Geology and Morphodynamics of a Tidal Flat Area Along the German North Sea Coast, Die Küste, Heft 69, 2005.

ROELVINK, J. A. and VAN BANNING, G. K. F. M.: Design and Development of DELFT3D and Application to Coastal Morphodynamics, Hydroinformatics '94, Verwey, Minns, Babovic & Maksimovic [eds], Balkema, Rotterdam, pp. 451–455, 1994.

TORO, F.; MAYERLE, R.; POERBANDONO and WILKENS, J.: Patterns of Hydrodynamics in a Tide-Dominated Coastal Area in the South-Eastern German Bight, Die Küste, Heft 69, 2005.

VAN RIJN, L. C.; WALSTRA, D. J. R.; GRASMEIJER, B.; SUTHERLAND, J.; PAN, S. and Sierra, J. P.: Simulation of Nearshore Hydrodynamics and Morphodynamics on the Time Scale of Storms and Seasons Using Process-Based Profile Models. In Van Rijn, L. C., B. G. Ruessink and J. P. M. Mulder (ed.), The Behaviour of a Straight Sandy Coast on the Time Scale of Storms and Seasons: Process Knowledge and Guidelines for Coastal Management: End Document March 2002. EC MAST Project, MAS3- CT97-0086 COAST3D – EGMOND, 2002.

WALSTRA, D. J. R.; VAN RIJN, L.; BLOGG, H. and VAN ORMONDT, M.: Evaluation of a hydrodynamic area model based on the COAST3D data at Teignmouth 1999. Paper D4 of: COAST3D Final Volume of Summary Papers. Report TR121, HR Wallingford, UK, pp D4.1-D4.4, 2001.

WILKENS, J.: Medium Scale Morphodynamics of the Central Dithmarschen Bight, Ph.D. thesis, University of Kiel, Germany, (available under http://e-diss.uni-kiel.de/diss_1369/d1369.pdf), 2004.

WILKENS, J.; JUNGE, I. and HOYME, H.: Modelling of Waves in a Tidal Flat Area in the South-Eastern German Bight, Die Küste, Heft 69, 2005.